A COMPARISON OF TIME-SWITCHED TRANSMIT DIVERSITY AND SPACE-TIME CODED SYSTEMS OVER TIME-VARYING MISO CHANNELS

A THESIS SUBMITTED TO
THE GRADUATE SCHOOL OF NATURAL AND APPLIED SCIENCES
OF
MIDDLE EAST TECHNICAL UNIVERSITY

BY

ERMAN KÖKEN

IN PARTIAL FULFILLMENT OF THE REQUIREMENTS
FOR
THE DEGREE OF MASTER OF SCIENCE
IN
ELECTRICAL AND ELECTRONICS ENGINEERING

SEPTEMBER 2011

Approval of the thesis:

A COMPARISON OF TIME-SWITCHED TRANSMIT DIVERSITY AND SPACE-TIME CODED SYSTEMS OVER TIME-VARYING MISO CHANNELS

submitted by **ERMAN KÖKEN** in partial fulfillment of the requirements for the degree of **Master of Science in Electrical and Electronics Engineering Department, Middle East Technical University** by,

Prof. Dr. Canan Özgen
Dean, Graduate School of **Natural and Applied Sciences** _____

Prof. Dr. İsmet Erkmen
Head of Department, **Electrical and Electronics Engineering** _____

Assoc. Prof. Dr. Ali Özgür Yılmaz
Supervisor, **Electrical and Electronics Engineering Dept., METU** _____

Examining Committee Members:

Prof. Dr. Yalçın Tanık
Electrical and Electronics Engineering, METU _____

Assoc. Dr. Ali Özgür Yılmaz
Electrical and Electronics Engineering, METU _____

Prof. Dr. Mete Severcan
Electrical and Electronics Engineering, METU _____

Assoc. Dr. Çağatay Candan
Electrical and Electronics Engineering, METU _____

Celal Dudak, M.Sc.
Tübitak UZAY _____

Date: _____

I hereby declare that all information in this document has been obtained and presented in accordance with academic rules and ethical conduct. I also declare that, as required by these rules and conduct, I have fully cited and referenced all material and results that are not original to this work.

Name, Last Name: ERMAN KÖKEN

Signature :

ABSTRACT

A COMPARISON OF TIME-SWITCHED TRANSMIT DIVERSITY AND SPACE-TIME CODED SYSTEMS OVER TIME-VARYING MISO CHANNELS

Köken, Erman
M.Sc., Department of Electrical and Electronics Engineering
Supervisor : Assoc. Prof. Dr. Ali Özgür Yılmaz

September 2011, 78 pages

This thesis presents a comparison between two transmit diversity schemes, namely space-time coding and time-switched transmit diversity (TSTD) over block-fading and time-varying multi-input single-output (MISO) channels with different channel parameters. The schemes are concatenated with outer channel codes in order to achieve spatio-temporal diversity. The analytical results are derived for the error performances of the systems and the simulation results as well as outage probabilities are provided. Besides, the details of the pilot-symbol-aided modulation (PSAM) technique are investigated and the error performances of the systems are analyzed when the channel state information is estimated with PSAM. It is demonstrated using the analytical and simulation results that TSTD have a comparable error performance with the space-time coding techniques and it even outperforms the space-time codes for some channel parameters. Our results indicate that TSTD can be suggested as an alternative to space-time codes in some time-varying channels especially due to the implementation simplicity.

Keywords: space-time coding, TSTD, PSAM, block-fading, time-varying channel

ÖZ

ZAMAN ANAHTARLAMALI GÖNDERİM ÇEŞİTLEMESİ VE UZAY-ZAMAN KODLU SİSTEMLERİN ZAMANDA DEĞİŞKEN ÇOK-GİRDİLİ TEK-ÇIKTILI KANALLARDAKİ KARŞILAŞTIRMASI

Köken, Erman
Yüksek Lisans, Elektrik ve Elektronik Mühendisliği Bölümü
Tez Yöneticisi : Doç. Dr. Ali Özgür Yılmaz

Eylül 2011, 78 sayfa

Çalışmada iki gönderim çeşitleme tekniği, uzay-zaman kodlaması ve zaman anahtarlamalı gönderim çeşitlemesi (TSTD), blok sönümlemeli ve zamanda değişken sürekli sönümlemeli çok-girdili tek-çıktılı (MISO) kanallarda kanal parametreleri ile karşılaştırılmıştır. Gönderim çeşitleme teknikleri, uzay-zamansal çeşitlemeyi elde etmek amacıyla kanal kodlarıyla birlikte kullanılmıştır. Sistemlerin hata başarımlarının analitik olarak incelenmiş, simülasyon sonuçları ve kesinti olasılıkları da çalışmada verilmiştir. Ayrıca, pilot sembol yardımlı kipleme (PSAM) ayrıntılı biçimde incelenmiş ve sistemlerin PSAM kullanıldığı durumdaki başarımı da analiz edilmiştir. TSTD'nin uzay-zaman kodlar ile yakın başarım sağladığı hatta bazı durumlarda daha iyi çalıştığı, analitik ve simülasyon sonuçları ile gösterilmiştir. Böylece, kolaylıkla uygulanabilen TSTD tekniğinin zamanda değişken sönümlemeli kanallarda uzay-zaman kodlarına alternatif olabileceği gösterilmiştir.

Anahtar Kelimeler: uzay-zaman kodlama, TSTD, PSAM, blok sönümleme, zamanda değişken kanal

ACKNOWLEDGMENTS

I would like to express my sincere thanks to my supervisor Assoc.Prof.Dr. Ali Özgür Yılmaz for his continuing encouragement, patience, and guidance. I consider studying with him as a great privilege. He is not only a mentor of research and scholarship for me, but also a mentor of life.

I was very fortunate to meet such good fellows such as Tuğcan Aktaş and Gökhan Muzaffer Güvensen. I appreciate their invaluable contributions to my academic and personal life. Sincerely, my graditute for them is beyond the words and I feel truly indebted to them. Special thanks go to Alper Bereketli and Cüneyt Baykal for the cheerful moments we have shared.

I wish to thank my valued, understanding, and helpful friends at the Telecommunications Laboratory Neyre Tekbıyık, Seçil Özdemir, Mehmet Fatih Özçelik, Mehmet Akif Antepli, and our laboratory technician Oktay Koç. Also Muhammet Fatih Bayramoğlu must be mentioned for advising me as a senior student and for being a close friend for over ten years.

I would also like to thank Burak Eminoğlu and other colleagues at the Analog and Digital Electronics Laboratory. I must acknowledge their assistance in my teaching experience.

I am also grateful to The Scientific and Technological Research Council of Turkey, TÜBİTAK, for the financial support that I have benefited from during the first year of my study.

Finally, I wish to thank my beloved parents and my brother for always standing by me and their endless support.

TABLE OF CONTENTS

LIST OF TABLES

TABLES

LIST OF FIGURES

FIGURES

CHAPTER 1

INTRODUCTION

The employment of multiple antennas for wireless communication systems has gained a substantial interest after the landmark paper [1] demonstrated that multiple-antenna wireless communication links promise very high data rates with low error probabilities. Utilization of multiple antennas can either enable increasing the data rate with the aid of spatial-multiplexing or increasing the spatial diversity by transmitting redundant signals on different transmit antennas and collecting the replicas of the signal at different receive antennas. Some examples of the spatial multiplexing techniques are Bell Labs Layered Space-Time (BLAST) architectures, i.e., vertical BLAST (V-BLAST) and diagonal BLAST (D-BLAST) [2]. Receive diversity techniques have been well-documented since 1950s, whereas the transmit diversity techniques emerged in late 1990s with space-time codes. Two prominent examples of the space-time codes are the space-time trellis codes (STTC) [3] and the space-time block codes (STBC) [1].

STBC's have attracted huge interest due to the linear processing in the receiver which renders simple detection available. Being the only full-rate STBC, the Alamouti scheme [4] is widely used and has been accepted in telecommunication standards such as UMTS, WiMAX, etc.

Albeit the benefits of the space-time codes, their implementations as well as of other MIMO systems have certain drawbacks. For example, multiple RF-chains are required which leads to an increased cost. Furthermore, the employment of multiple RF-chains may entail more sensitivity against the impairments encountered in practice.

The time-switched transmit diversity (TSTD) technique was proposed in [5] and offers a low cost implementation for achieving transmit diversity due to its capability of being implemented with a single RF-chain. Especially used in the synchronization channels of UMTS

systems, the capabilities and the advantages of the TSTD technique over the STBC's should be investigated. This thesis mainly discussed this issue and compares the error performances of two transmit diversity schemes, namely TSTD and the Alamouti scheme, under certain conditions such as channel estimation imperfections, variation of the channel gain coefficients in time, etc.

The thesis is organized as follows. In Chapter 2 the important features of space-time codes are provided. The quasi-static MIMO channel model is explained and the MIMO capacity as well as the space-time code design criteria are provided. We elaborate on the encoding and detection structures of the STBC's with two transmit antennas, namely the Alamouti scheme and differential space-time block codes (DSTBC). Moreover, other space-time codes that are studied in the literature are mentioned.

Chapter 3 is devoted to the comparison of TSTD and STBC systems over 2x1 MISO block-fading channels. Both concatenated with blockwise maximum distance separable (MDS) convolutional codes, the error performances of the transmit diversity schemes are compared with different numbers of block realizations. The simulations are verified with the analytical results and the outage probabilities of the techniques are given. The comparison is also done with differential techniques, i.e., TSTD with DPSK and DSTBC.

The main features of a channel estimation technique widely used for time-varying flat-fading channels, namely PSAM, are explained in Chapter 4. The performance of the technique is provided with different channel parameters such as Doppler spread, pilot spacing and number of interpolators. The detrimental effects of time-variation and channel estimation error on the performances of the Alamouti scheme and DSTBC with two transmit antennas are demonstrated with simulation and analytical results.

In Chapter 5 the detrimental effects of the time-variation and the channel estimation error on the performances of the coherent and differential transmit diversity schemes concatenated with convolutional codes over time-varying 2x1 MISO channels are investigated. The spatio-temporal diversity provided by the time-varying channel is exploited by using the encoding structures that are designed for block-fading channels and that are explained in Chapter 3. The comparison is performed with different channel parameters and TSTD is shown to have better performance than STBC with two transmit antennas under some conditions.

In Chapter 6 we point out the main points and conclude the thesis.

CHAPTER 2

SPACE-TIME CODES

2.1 MIMO Transmission Model

We consider a discrete-time symbol model for a narrowband multi-input multi-output (MIMO) wireless communication system in which N_t transmit antennas and N_r receive antennas are employed. At each time epoch t, the signals x_{ti} $(1 \leq i \leq N_t)$ are transmitted simultaneously each from the ith transmit antenna. At time t, the signal received at the jth receive antenna is the sum of the symbols sent from the transmitters scaled by a multiplicative channel gain and perturbed by complex Gaussian noise. Along with a rich scattering environment, the antenna spacing is assumed to be large enough so that the channel gain coefficients between transmit and receive antennas are independent. The coefficient h_{ij} represents the unit power Rayleigh distributed channel gain between the ith transmit antenna and the jth receive antenna. The probability density function (pdf) of h_{ij} is

$$p\left(h_{ij}\right) = \frac{1}{\pi} e^{-\left|h_{ij}\right|^2} \tag{2.1}$$

for all i and j. The received signal at time t at the jth receive antenna can be represented as

$$y_{tj} = \sqrt{\frac{E_s}{N_t}} \sum_{i=1}^{N_t} h_{ij} x_{ti} + n_{tj} \tag{2.2}$$

where n_{tj} denotes spatially and temporally white zero mean circularly symmetric complex Gaussian noise samples observed at the jth receive antenna at time t. Each noise sample has a variance $N_0/2$ per dimension. The energy of symbols are confined to

$$\sum_{i=1}^{N_t} E\left\{|s_{it}|^2\right\} = E_s \tag{2.3}$$

for all t. Hence the transmit energy at each epoch is E_s. We assume that the channel is quasi-static, i.e., the channel gain coefficients are constant for a long time and then change independently. We also assume that the channel is frequency nonselective.

For convenience, we will put the signals within T symbol durations (epochs) and the corresponding gain coefficients into a matrix form. Since the channel is quasi-static, the channel gain coefficients are assumed to be constant for $1 \leq t \leq T$. The transmission model where the noise is normalized, i.e., $N_0 = 1$, is given as

$$\mathbf{Y} = \sqrt{\frac{\gamma}{N_t}}\mathbf{X}\mathbf{H} + \mathbf{N} \tag{2.4}$$

where

$$\mathbf{X} = \begin{bmatrix} x_{11} & x_{12} & \dots & x_{1N_t} \\ x_{21} & x_{22} & \cdots & x_{2N_t} \\ \vdots & \vdots & \ddots & \vdots \\ x_{T1} & x_{T2} & \cdots & x_{TN_t} \end{bmatrix} \in \mathbb{C}^{T \times N_t} \tag{2.5}$$

is the transmitted symbol matrix,

$$\mathbf{H} = \begin{bmatrix} h_{11} & h_{12} & \dots & h_{1N_r} \\ h_{21} & h_{22} & \cdots & h_{2N_r} \\ \vdots & \vdots & \ddots & \vdots \\ h_{N_t1} & h_{N_t2} & \cdots & h_{N_tN_r} \end{bmatrix} \in \mathbb{C}^{N_t \times N_r} \tag{2.6}$$

is the channel gain matrix,

$$\mathbf{Y} = \begin{bmatrix} y_{11} & y_{12} & \dots & y_{1N_r} \\ y_{21} & y_{22} & \cdots & y_{2N_r} \\ \vdots & \vdots & \ddots & \vdots \\ y_{T1} & y_{T2} & \cdots & y_{TN_r} \end{bmatrix} \in \mathbb{C}^{T \times N_r} \tag{2.7}$$

is the received signal matrix and

$$\gamma = \frac{E_s}{N_0} \tag{2.8}$$

is the signal-to-noise ratio (SNR).

We only investigate an open-loop system, i.e., the channel state information (CSI) is not available at the transmitter and there is no feedback link. We will assume that the channel state information is perfectly known at the receiver up until Section 2.5.

2.2 MIMO Capacity

In [2, 1], it is shown that coherent MIMO channels offer a substantial increase in the capacity. In a quasi-static fading channel with independent fading paths where the CSI is perfectly known at the receiver side but not known by the transmitter, the capacity-achieving probability density function (pdf) of input signal at each transmit antenna is shown to be that of independent zero mean circularly symmetric Gaussian distribution with equal energy.

The ergodic capacity of the MIMO channel is

$$C_{erg} = \mathcal{E}\left\{\log_2\left(\det\left(I_{N_r} + \frac{\gamma}{N_t}\mathbf{H}^H\mathbf{H}\right)\right)\right\} \tag{2.9}$$

where $\mathcal{E}\{.\}$ is the expectation operator. The expectation is evaluated in [1] as

$$C_{erg} = \int_0^\infty log_2\left(1 + \frac{\gamma}{N_t}\zeta\right)\sum_{k=0}^{N_1-1}\frac{k!}{(k+N_2-N_1)!}\left(L_k^{N_2-N_1}(\zeta)\right)^2\zeta^{N_2-N_1}e^{-\zeta}d\zeta \tag{2.10}$$

where

$$L_k^A(\zeta) = \frac{1}{k!}e^{\zeta}\zeta^A\frac{d^k}{d\zeta^k}\left(e^{-\zeta}\zeta^{A+k}\right) \tag{2.11}$$

is the associated Laguerre polynomial of order k, $N_2 = \max(N_t, N_r)$, and $N_1 = \min(N_t, N_r)$.

When $N_r = 1$, the law of large numbers implies as N_t increases that

$$\frac{1}{N_t}\mathbf{H}^H\mathbf{H} \to 1. \tag{2.12}$$

Hence for large N_t, the capacity can be expressed as

$$C_{erg} \approx \log_2(1+\gamma) \tag{2.13}$$

which is approximately equal to the additive white Gaussian noise (AWGN) channel capacity. In [6], the capacity is approximated in high SNR as

$$C \approx \min(N_t, N_r)\log_2\left(\frac{\gamma}{N_t}\right) + \sum_{k=|N_t-N_r|+1}^{\min(N_t,N_r)} \log_2 \chi_k \tag{2.14}$$

where χ_k is a chi-square random variable with $2k$ degrees of freedom.

Equation (2.14) implies that the capacity increases by $\min(N_t, N_r)$ bits per channel use at high SNR with each 3 dB increase in the SNR.

The channel capacity of MIMO channel when the channel state information is not available at either side is discussed in Section 2.6.

2.3 Space-Time Code Design Criteria

Following the notation in (2.4), we can express the maximum likelihood (ML) detector in MIMO channel as

$$\hat{\mathbf{X}} = \arg\max_{\mathbf{X}^i} \; p\left(\mathbf{Y} \mid \mathbf{X}^i, \mathbf{H}\right) \tag{2.15}$$

where the conditional probability is

$$p\left(\mathbf{Y} \mid \mathbf{X}^i, \mathbf{H}\right) = \frac{1}{(\pi N_0)^{TN_r}} \exp\left(-\mathrm{tr}\left(\left(\mathbf{Y} - \sqrt{\frac{E_s}{N_t}}\mathbf{X}^i\mathbf{H}\right)^H\left(\mathbf{Y} - \sqrt{\frac{E_s}{N_t}}\mathbf{X}^i\mathbf{H}\right)\right)\right) \tag{2.16}$$

in which tr(.) is the trace operator.

Since it is cumbersome to track the probability of error, it is convenient to analyze the pairwise error probability (PEP) between two codewords. The PEP between any two codewords $\mathbf{X^k}$and $\mathbf{X^m}$ is provided in [3] as

$$PEP\left(\mathbf{X^k} \rightarrow \mathbf{X^m} \mid \mathbf{H}\right) = Q\left(\sqrt{\frac{\gamma}{2N_t}\mathrm{tr}\left(\left(\mathbf{D_{km}H}\right)^H\left(\mathbf{D_{km}H}\right)\right)}\right) \tag{2.17}$$

where $\mathbf{D_{km}} = \mathbf{X^m} - \mathbf{X^k}$.

Average PEP can be found by averaging the conditional PEP in (2.17) over all channel realizations:

$$PEP\left(\mathbf{X^k} \rightarrow \mathbf{X^m}\right) = E_{\mathbf{H}}\left(PEP\left(\mathbf{X^k} \rightarrow \mathbf{X^m} \mid \mathbf{H}\right)\right). \tag{2.18}$$

For high SNR a tight upper bound in high SNR is derived in [3] as

$$PEP\left(\mathbf{X^k} \rightarrow \mathbf{X^m}\right) \leq \frac{4^{rN_r}}{\left(\prod_{n=1}^{r}\lambda_n\right)^{N_r}\gamma^{rN_r}} \tag{2.19}$$

where r is the rank of $\mathbf{D_{km}}$ and $\lambda_n^{\mathbf{km}}$'s are the non-zero eigenvalues of $\mathbf{A_{km}} = \mathbf{D_{km}}^H\mathbf{D_{km}}$. For high SNR, any PEP in fading channels can be approximated as [7]

$$PEP\left(\mathbf{X^k} \rightarrow \mathbf{X^m}\right) \approx \left(G_c^{\mathbf{km}}\frac{\gamma}{4N_t}\right)^{-G_d^{\mathbf{km}}} \tag{2.20}$$

in which $G_c^{\mathbf{km}}$ is represents coding gain and $G_d^{\mathbf{km}}$ represents diversity gain of PEP between $\mathbf{X^k}$ and $\mathbf{X^m}$. Following this approximation, diversity and coding gains are compactly given as

$$G_d^{\mathbf{km}} = N_r\mathrm{rank}\ \mathbf{D_{km}}, \tag{2.21}$$

$$G_c^{\mathbf{km}} = \left(\prod\lambda_n\right)^{\mathrm{rank}\ \mathbf{D_{km}}}. \tag{2.22}$$

Considering PEP's between all of the codewords, the overall diversity gain is

$$G_d = \min_{\mathbf{k}\neq\mathbf{m}} G_d^{\mathbf{km}} \tag{2.23}$$

and the overall coding gain is

$$G_c = \min_{\mathbf{k}\neq\mathbf{m};G=G_d} G_c^{\mathbf{km}}. \tag{2.24}$$

Based on these results the following criteria are proposed to design space time codes:

- In order to increase *the diversity gain*, the minimum of rank $\mathbf{D_{km}}$ should be maximized over all $\mathbf{k} \neq \mathbf{m}$.
- In order to increase *the coding gain*, the product of $\lambda_n^{\mathbf{km}}$'s should be maximized over all $\mathbf{k} \neq \mathbf{m}$ with minimum diversity.

If G_d equals to $N_t N_r$, the space time code is said to be full diversity.

2.4 Space-Time Block Codes

Space-time block codes are designed to achieve full diversity with a simple encoding structure and low decoding complexity. A sequence of P symbols $s_1, s_2, .., s_P$, that are elements of a specific constellation set such as phase shift keying (PSK) or quadrature amplitude modulation (QAM), are mapped into a TxN_t transmitted matrix $\mathbf{X}$ entries of which are the linear combinations of $s_1, s_2, .., s_P$ (and $s_1^*, s_2^*, .., s_P^*$ if a complex constellation is chosen). This mapping operation is referred to as space-time block encoding. The symbol rate is denoted as R with

$$R = \frac{P}{T} \tag{2.25}$$

symbols per channel use. If R equals one, the code will be declared as a full-rate or rate-one code. The criteria in Section 2.3 indicates that the design of transmitted signals does not depend on the number of receive antennas. Multiple receive antennas provide only additional diversity gain with a very simple decoding structure.

STBC's are usually designed with the orthogonality property [8] so that the detection of the symbols $s_1, s_2, .., s_P$ are decoupled with a simple linear processing and the decision statistics are obtained separately for each symbol. STBC's are aimed to achieve full-diversity with a

rate as large as possible. A comprehensive description of STBC's and their properties can be found in [8].

2.4.1 Alamouti Scheme

The Alamouti scheme [4] is a full-rate full-diversity (FRFD) orthogonal STBC (OSTBC) with $N_t = 2$ and $T = 2$. The transmitted signal matrix is

$$\mathbf{X} = \mathbf{S}(s_1, s_2) = \begin{bmatrix} s_1 & s_2 \\ -s_2^* & s_1^* \end{bmatrix} \tag{2.26}$$

where s_1 and s_2 are elements of a specific constellation set. For the moment, we will assume that $N_r = 1$. Ignoring the receive antenna index j, (2.4) becomes

$$\begin{bmatrix} y_1 \\ y_2 \end{bmatrix} = \sqrt{\frac{E_s}{2}} \begin{bmatrix} s_1 & s_2 \\ -s_2^* & s_1^* \end{bmatrix} \begin{bmatrix} h_1 \\ h_2 \end{bmatrix} + \begin{bmatrix} n_1 \\ n_2 \end{bmatrix}. \tag{2.27}$$

We will derive the ML estimations of s_1 and s_2. The estimated symbols can be found from

$$(\hat{s}_1, \hat{s}_2) = \arg\min_{s_1, s_2} \left\{ \left| y_1 - \sqrt{\frac{E_s}{2}} (h_1 s_1 - h_2 s_2) \right|^2 + \left| y_2 - \sqrt{\frac{E_s}{2}} \left(h_2 s_1^* - h_1 s_2^* \right) \right|^2 \right\} \tag{2.28}$$

which corresponds to

$$(\hat{s}_1, \hat{s}_2) = \arg\min_{s_1, s_2} \left| E_{s,h} s_1 - \left(h_1^* y_1 + h_2 y_2^* \right) \right|^2 + \left| E_{s,h} s_2 - \left(h_2^* y_1 - h_1 y_2^* \right) \right|^2 \tag{2.29}$$

where $E_{s,h}$ equals to $\left(|h_1|^2 + |h_2|^2 \right) \sqrt{\frac{E_s}{2}}$. This suggests that the statistics for $\hat{s}_1$ and $\hat{s}_2$ can be obtained separately. Eq. 2.27 can also be rewriten as

$$\begin{bmatrix} y_1 \\ y_2^* \end{bmatrix} = \sqrt{\frac{E_s}{2}} \Theta \begin{bmatrix} s_1 \\ s_2 \end{bmatrix} + \begin{bmatrix} n_1 \\ n_2 \end{bmatrix} \tag{2.30}$$

where

$$\Theta = \begin{bmatrix} h_1 & h_2 \\ h_2^* & -h_1^* \end{bmatrix}. \tag{2.31}$$

Note that the columns of Θ are orthogonal, thus

$$\begin{bmatrix} r_1 \\ r_2 \end{bmatrix} = \mathbf{\Theta}^H \begin{bmatrix} y_1 \\ y_2^* \end{bmatrix} = E_{s,h} I \begin{bmatrix} s_1 \\ s_2 \end{bmatrix} + \begin{bmatrix} \tilde{n}_1 \\ \tilde{n}_2 \end{bmatrix} \tag{2.32}$$

where $\tilde{n}_1$ and $\tilde{n}_2$ are independent Gaussian variables obeying $C\mathcal{N}\left(0, \left(|h_1|^2 + |h_2|^2\right) N_0\right)$.

Now let us consider the case with $N_r > 1$

$$\begin{bmatrix} r_1 \\ r_2 \end{bmatrix} = \sum_{j=1}^{N_r} \begin{bmatrix} r_{1j} \\ r_{2j} \end{bmatrix} \tag{2.33}$$

where

$$\begin{bmatrix} r_{1j} \\ r_{2j} \end{bmatrix} = \mathbf{\Theta}_j^H \begin{bmatrix} y_{1j} \\ y_{2j}^* \end{bmatrix} \tag{2.34}$$

$$\Theta_j = \begin{bmatrix} h_{1j} & h_{2j} \\ h_{2j}^* & -h_{1j}^* \end{bmatrix}. \tag{2.35}$$

$$\begin{bmatrix} r_1 \\ r_2 \end{bmatrix} = E_{s,H} I \begin{bmatrix} s_1 \\ s_2 \end{bmatrix} + \begin{bmatrix} \tilde{w}_1 \\ \tilde{w}_2 \end{bmatrix} \tag{2.36}$$

where $E_{s,H} = \sum_{j=1}^{N_r} \left(\left|h_{1j}\right|^2 + \left|h_{2j}\right|^2\right) \sqrt{\frac{E_s}{2}}$. Note that (2.33) corresponds to maximum ratio combining.

The uncoded BPSK error probability for the Alamouti scheme is [6]

$$P_s = \frac{1}{2}\left(1 - \sqrt{\frac{\gamma}{\gamma+2}} \sum_{c=0}^{2N_r-1} \begin{pmatrix} 2c \\ c \end{pmatrix} \left(\frac{1}{2(\gamma+2)}\right)^c\right) \tag{2.37}$$

Since generalization to multiple receive antenna case is straight forward, we will assume that $N_r = 1$ in the next two subsections.

2.4.2 Orthogonal STBC

Note that the facility to extract the statistics for symbols separately is due to the orthogonality of the columns of Θ, which is in turn due to the orthogonality of the columns of $\mathbf{X}$. If the symbols $s_1, s_2, ..., s_P$ are elements of a real constellation set like pulse amplitude modulation (PAM) or binary phase shift keying (BPSK), it is shown in [8] that for any N_t, a FRFD orthogonal STBC (OSTBC) can be found for a suitable T, as a function of N_t, with the aid of orthogonal signal sets. Although it is possible to find FRFD OSTBC's using real constellations for any N_t, there are bounds on symbols per channels use R of the full-diversity OSTBC's when we extend the constellation to complex domain. It is shown in [9] that R is upper-bounded by 3/4 for full-diversity OSTBC if $N_t > 2$.

2.4.3 Other Space-Time Codes

Space time trellis codes (STTC) [3] were proposed in 1998. It can be considered as the generalization of trellis coded modulation (TCM) to multiple antenna systems. Main disadvantage of the scheme is that the complexity of the trellis decoder increases exponentially with the transmission rate and the antenna number.

Since it is not possible to generate FRFD OSTBC's for complex constellations, STBC's that are not orthogonal are also considered in the literature. In [10], quasi-orthogonal STBC's are proposed. Some columns are not pairwise orthogonal, and this renders separate decoding impossible. Moreover QOSTBC cannot attain full diversity unless some of the symbols are rotated[11]. Threaded algebraic STBC which is a generalization of the BLAST architecture [12] and space-time shift keying [13] may be given as other examples.

2.5 Differential Space-Time Block Codes

Differential STBC [14] can be considered as a generalization of differential phase shift keying (DPSK) to multiple transmit antenna case. Similar to DPSK, differential STBC systems does not need CSI neither at the transmitter not at the receiver side. Since the generalization of multiple receive antenna case is straightforward as in the coherent STBC, we will assume $N_r = 1$ without loss of generality.

For $N_t = 2$, two input symbols, s_t and s_{t+1}, that are from a PSK constellation, are mapped into an A, B pair. This mapping is not unique. Different mappings with the same error performance may lead to different transmitted symbol constellations.

$$A = (s_t + s_{t+1})/2, \; B = \left(-s_{t+1}^* + s_t^*\right)/2. \tag{2.38}$$

Symbols are differentially encoded based on the A, B pair with

$$\begin{bmatrix} c_t \\ c_{t+1} \end{bmatrix} = A \begin{bmatrix} c_{t-2} \\ c_{t-1} \end{bmatrix} + B \begin{bmatrix} -c_{t-1}^* \\ c_{t-2}^* \end{bmatrix}. \tag{2.39}$$

Note that c_t 's are always on the same constellation with s_t, which is a result of the mapping, i.e., for a mapping other than given in (2.38) with the same error performance, differentially encoded symbols would not be on the unit circle. The codeword matrix that is to be transmitted within time t and $t+1$ is

$$\mathbf{X} = \begin{bmatrix} c_t & c_{t+1} \\ -c_{t+1}^* & c_t^* \end{bmatrix}. \tag{2.40}$$

This part of the encoding is equivalent to coherent Alamouti transmission scheme.

Since the symbols are differentially encoded with respect to two previous symbols, the estimation is performed using four observations, $\mathbf{r} = [r_{t-2} r_{t-1} r_t r_{t+1}]^T$. The equation for the received vector in a compact form is

$$\begin{bmatrix} r_{t-2} \\ r_{t-1}^* \\ r_t \\ r_{t+1}^* \end{bmatrix} = \sqrt{\frac{E_s}{2}} \begin{bmatrix} h_1 & h_2 & 0 & 0 \\ h_2^* & -h_1^* & 0 & 0 \\ 0 & 0 & h_1 & h_2 \\ 0 & 0 & h_2^* & -h_1^* \end{bmatrix} \begin{bmatrix} c_{t-2} \\ c_{t-1} \\ c_t \\ c_{t+1} \end{bmatrix} + \begin{bmatrix} n_{t-2} \\ n_{t-1}^* \\ n_t \\ n_{t+1}^* \end{bmatrix}. \tag{2.41}$$

The pair is found with the ML receiver:

$$\left(\hat{A}, \hat{B}\right) = \arg\max_{A,B} p\left(\mathbf{r} \mid A, B\right) \tag{2.42}$$

where the conditional probability equals to

$$p\left(\mathbf{r} \mid A, B\right) = \frac{1}{|\pi \mathbf{R}|} e^{-\mathbf{r}^H \mathbf{R}^{-1} \mathbf{r}}. \tag{2.43}$$

The autocorrelation function $\mathbf{R}$ is a function of A, B, E_s, and N_0

$$\mathbf{R} = \mathcal{E}\left\{\mathbf{r}\mathbf{r}^H\right\} = N_0 \begin{bmatrix} \gamma+1 & 0 & \gamma A^* & -\gamma B \\ 0 & \gamma+1 & \gamma B^* & \gamma A \\ \gamma A & \gamma B & \gamma+1 & 0 \\ -\gamma B^* & \gamma A^* & 0 & \gamma+1 \end{bmatrix}. \tag{2.44}$$

Using the matrix property [15]

$$\begin{bmatrix} \alpha I & M \\ M & \alpha I \end{bmatrix}^{-1} = \begin{bmatrix} \left(\alpha I - \frac{MM^H}{\alpha}\right)^{-1} & -\left(\alpha I - \frac{MM^H}{\alpha}\right)^{-1} \frac{M}{\alpha} \\ -\frac{M^H}{\alpha}\left(\alpha I - \frac{MM^H}{\alpha}\right)^{-1} & \frac{I}{\alpha} + \frac{M^H}{\alpha}\left(\alpha I - \frac{MM^H}{\alpha}\right)^{-1} \frac{M}{\alpha} \end{bmatrix} \tag{2.45}$$

with

$$\alpha = \gamma + 1, M = \begin{bmatrix} \gamma A^* & -\gamma B \\ \gamma B^* & \gamma A \end{bmatrix}, \tag{2.46}$$

the inverse of $\mathbf{R}$, $\mathbf{R}^{-1}$, can be found as

$$\mathbf{R}^{-1} = \frac{1}{N_0} \begin{bmatrix} \frac{\gamma+1}{2\gamma+1} & 0 & -\frac{\gamma}{2\gamma+1}A^* & \frac{\gamma}{2\gamma+1}B \\ 0 & \frac{\gamma+1}{2\gamma+1} & -\frac{\gamma}{2\gamma+1}B^* & -\frac{\gamma}{2\gamma+1}A \\ -\frac{\gamma}{2\gamma+1}A & -\frac{\gamma}{2\gamma+1}B & \frac{\gamma+1}{2\gamma+1} & 0 \\ \frac{\gamma}{2\gamma+1}B^* & -\frac{\gamma}{2\gamma+1}A^* & 0 & \frac{\gamma+1}{2\gamma+1} \end{bmatrix}. \tag{2.47}$$

Note that the determinant of $\mathbf{R}$, $|\mathbf{R}|$,is equal for all A,B pairs. Therefore

$$\left(\hat{A}, \hat{B}\right) = \arg\min_{A,B} \mathbf{r}^H \mathbf{R}^{-1} \mathbf{r} \tag{2.48}$$

as γ goes to infinity. Assuming SNR is high, Eq. 2.48 becomes

$$\left(\hat{A}, \hat{B}\right) = \arg\min_{A,B} \left(|R_A - A|^2 + |R_B - B|^2\right) \tag{2.49}$$

where

$$R_A = r^*_{t-2} r_t + r_{t-1} r^*_{t+1},$$
$$R_B = -r^*_{t-1} r_t + r_{t-2} r^*_{t+1}. \tag{2.50}$$

The A,B pair should be jointly detected. The statistics for symbols s_t and s_{t+1}, $\tilde{s}_t$ and $\tilde{s}_{t+1}$can be separately obtained by

$$\tilde{s}_t = R_A + R^*_B, \tilde{s}_{t+1} = R^*_B - R_A \tag{2.51}$$

which is the inverse of the mapping in (2.38).

This scheme achieves full diversity with full rate. Similar to the comparison of coherent PSK and DPSK, differential space time modulation with $N_t = 2$ has 3dB performance degradation as compared to the coherent Alamouti scheme. The bit error rates (BER) for the two schemes are depicted in Figure 2.5.

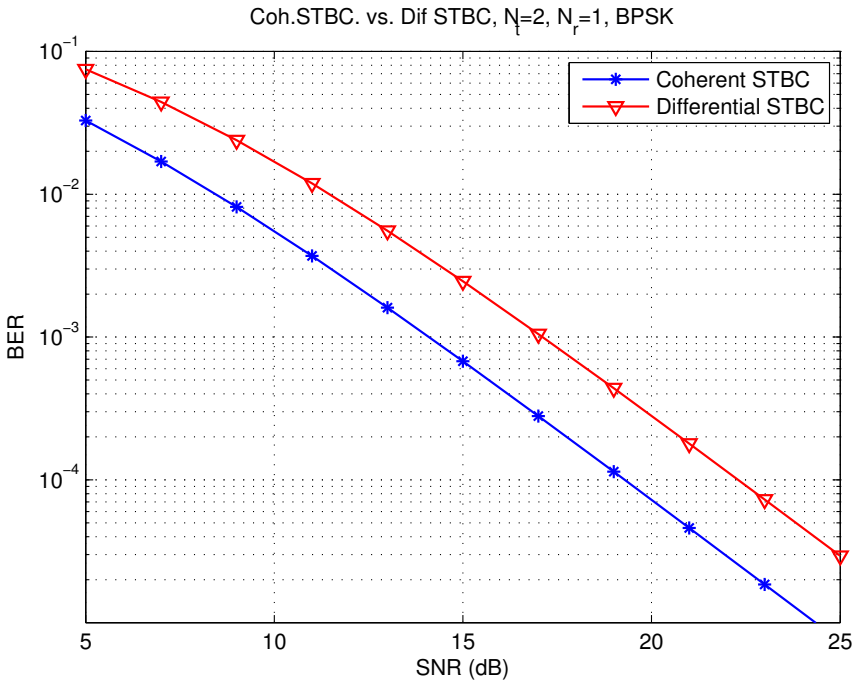

Figure 2.1: The performance resultes for coherent and differential STBCs

Generalization to multiple transmit antenna with $N_t > 2$ is investigated in [16]. By using a FRFD OSTBC with real constellation it is shown that a half rate full diversity differential

STBC can be generated with complex constellation for the same transmit antenna number. Systematic constructions for BPSK FRFD differential STBC's are also exist.

2.6 Unitary Space-Time Modulation

In [17] , capacity of a noncoherent MIMO system where the channel is constant for T symbol durations is analyzed. It is shown that an increase in N_t does not provide a capacity improvement if $N_t > T$. Moreover, capacity achieving input signals are shown to be the product of isotropically distributed unitary matrix and a diagonal real nonnegative matrix. Also in [18], a geometrical approach is suggested and the capacity is shown to increase by $V(1 - V/T)$ with each 3dB increase in SNR where $V = \min(N_t, N_r, \lfloor T/2 \rfloor)$. Inspired by the capacity achieving input distribution, unitary space-time modulation [19] and differential unitary space-time modulation [20] were proposed. An efficient receiver structure for diagonal unitary space-time modulation is given in [21] which has polynomial complexity in the number of antennas and rate. The complexity of the receiver of differential space-time modulation is exponential in the rate and number of antennas while differential STBC's in [14] and [16] possess linear decoding complexity.

2.7 Conclusion

In this chapter we gave some basic information about the space-time codes that are used in our scenarios in which we compare them with another transmit diversity technique. Space-time codes were proposed in late 1990's and since then there has been an extensive literature work on this subject. They rely on utilizing multiple transmit antennas and only optionally multiple receive antennas. Redundant replicas of data are transmitted in order to compensate for fading and noise so that spatial diversity the channel provides be achieved. Some of the space-time codes that are designed to achieve spatial diversity can also be used for achieving temporal diversity. Space-time codes are also extended to frequency selective channels, OFDM systems, and wireless networks in which distributed space-time codes are proposed.

CHAPTER 3

COMPARISON OF TSTD AND STBC OVER BLOCK-FADING MISO CHANNELS

In this chapter, we compare the performances of two transmit diversity schemes, namely, time-switched transmit diversity (TSTD) and the Alamouti scheme, both concatenated with an outer channel coding over multiple-input single-output (MISO) block-fading channels. The comparison is done in coherent and noncoherent channels with $N_t = 2$ transmit and $N_r = 1$ receive antennas. The performance analyses for BER, packet-error-rate (PER) and outage probabilities of two schemes are provided for coherent channels as well.

3.1 Coherent Block-Fading MISO Channels

In a MIMO block-fading (BF) channel with N_t transmit and N_r receive antennas, the channel gains are constant over L consecutive symbol durations and then change independently in each block. In order to exploit the spatio-temporal diversity the channel provides, channel coding (and interleaving if necessary) may be used. Codewords span a time duration occupying a number of blocks, namely B blocks. The B value may be constrained by the system allowances, frequency hopping rate, delay, etc.

The received signal at the jth receive antenna at time $(b-1)L+t$, y_{tj}^b is given as

$$y_{tj}^b = \sqrt{\frac{E_s}{N_t}} \sum_{i=1}^{N_t} h_{ij}^b x_{ti}^b + n_{tj}^b,\ 1 \le b \le B,\ 1 \le t \le L \tag{3.1}$$

where h_{ij}^b is the independent unit power Rayleigh distributed channel gain between the ith

transmit antenna and the jth receive antenna within bth block, n_{tj}^b denotes the noise sample received at the jth antenna at time $(b-1)L+t$ (at the bth block). The noise samples are independent samples of zero-mean circularly symmetric complex Gaussian (ZMCSCG) random variables each with variance $N_0/2$ per dimension. x_{ti}^b is the signal transmitted from ith antenna at time $(b-1)L+t$. Note that (3.1) can be put into matrix form as

$$\mathbf{Y}^b = \sqrt{\frac{\gamma}{N_t}}\mathbf{X}^b\mathbf{H}^b + \mathbf{N}^b,\ 1 \le b \le B \tag{3.2}$$

where $\mathbf{Y}^b$, $\mathbf{X}^b$, $\mathbf{H}^b$, and $\mathbf{N}^b$ are equivalent to $\mathbf{Y}$, $\mathbf{X}$, $\mathbf{H}$, and $\mathbf{N}$ respectively in 2.4 except with block index b and T replaced with L. Up until Section 3.9, we will assume that the CSI is perfectly known at the receiver, though not at the transmitter.

3.2 Time Switched Transmit Diversity

Time switched transmit diversity (TSTD) [5] is a technique which aims to achieve transmit diversity. TSTD is used in Universal Mobile Telecommunications System (UMTS) particularly on synchronization channels [22, 23, 24]. The main idea behind TSTD is to alternate the transmit antennas according to a predefined hopping pattern so that the data is transmitted from one antenna at a time. By using this technique, space diversity is turned into temporal diversity. The main advantage of TSTD is facilitating an implementation with only a single radio-frequency (RF) chain for multiple transmit antennas. The work in the thesis concentrate on 2x1 MISO BF channels without loss of generality, therefore we will give a quantitative explanation about the technique accordingly.

The signals are transmitted only on the 1st antenna during the first half of a block and only the 2nd antenna is activated during the second half. Thus the receiver signal at time $(b-1)L+t$ equals

$$y_t^b = \begin{cases} \sqrt{E_s}h_1^b x_t^b + n_t^b & 1 \le t \le L/2 \\ \sqrt{E_s}h_2^b x_t^b + n_t^b & L/2+1 \le t \le L \end{cases}. \tag{3.3}$$

With no loss of generality we will assume that all x_t^b's are elements of a specific constellation.

Note that, utilizing antenna hopping, a 2x1 MISO block fading channel with B independent

blocks each of which span L symbol durations is equivalent to a single-input single-output (SISO) block fading channel with $2B$ independent blocks each spanning $L/2$ symbol durations.

3.3 Alamouti Scheme

As explained in Section 2.4, two signals are mapped into a 2x2 transmission matrix and the matrix is sent within 2 symbol durations. The receiver signals at time $(b-1)L+t$ and $(b-1)L+t+1$ in a 2x1 channel are equal to

$$\begin{bmatrix} y_t^b \\ y_{t+1}^b \end{bmatrix} = \sqrt{\frac{E_s}{2}} \begin{bmatrix} x_t^b & x_{t+1}^b \\ -x_{t+1}^{b*} & x_t^{b*} \end{bmatrix} \begin{bmatrix} h_1^b \\ h_2^b \end{bmatrix} + \begin{bmatrix} n_t^b \\ n_{t+1}^b \end{bmatrix} \tag{3.4}$$

where t is an odd number. Note that the symbol pair are transmitted within the same block b.

3.4 Channel Coding and Interleaving

The purpose of channel coding is not seeking coding gain but rather exploiting the available diversity gain by extending the codeword such that it spans several blocks. To exemplify, TSTD transforms spatial diversity into temporal diversity and this diversity advantage can be benefitted from by using relevant channel coding and interleaving [25]. In the Alamouti scheme, the channel coding is expected to obtain only temporal diversity gain, since full spatial diversity is already gained.

The maximum achievable diversity gain d^* in a SISO-BF channel is upper-bounded by the generalized Singleton bound for finite constellations, which is shown below [25]:

$$d^* \leq 1 + \left\lfloor B\left(1 - \frac{R_b}{\log_2 |\mathcal{V}|}\right)\right\rfloor \tag{3.5}$$

where R_b is the bit rate, $\mathcal{V}$ is the constellation alphabet of the tranmitted symbols, and $|\mathcal{V}|$ is the cardinality of $\mathcal{V}$. In [26], the upper bound for the maximum achievable diversity gain for BPSK constellation on a N_txN_r MIMO channel is derived as

$$d^*_{N_t \mathrm{x} N_r} \leq N_r \left(1 + \left\lfloor N_t B \left(1 - \frac{R_b}{N_t}\right)\right\rfloor\right). \tag{3.6}$$

The transmit diversity techniques that we mention above further restrict the maximum achievable diversity. Using BPSK constellation, the upper bounds for the maximum achievable diversity in a 2x1 MISO channel, a TSTD system and an Alamouti encoded system are given as

$$d^*_{2\mathrm{x}1} \leq 1 + \left\lfloor 2B \left(1 - \frac{R_b}{2}\right)\right\rfloor, \tag{3.7}$$

$$d^*_{TSTD} \leq 1 + \lfloor 2B\,(1 - R_b)\rfloor, \tag{3.8}$$

$$d^*_{ALA} \leq 2\,(1 + \lfloor B\,(1 - R_b)\rfloor), \tag{3.9}$$

respectively.[1] Figure 3.4 depicts the upper bounds for achievable diversity gains when BPSK is used with $B = 4$. Note that, for any $B > 1$ and $R_b > 1/2B$, d_{MISO} is greater than d^*_{ALA} and d^*_{TSTD}. The three upper bounds are equal only if $R_b \leq 1/2B$.

In the following we explain the coding and interleaving structures that we used in order to compare TSTD and the Alamouti scheme.

A sequence of Q input bits $a_1 a_2 ... a_Q$ are convolutionally coded into $BL \log_2 |\mathcal{V}|$ bits $z_1 z_2 ... z_{BL \log_2 |\mathcal{V}|}$ with a coding rate $1/2B$, after the number of memory order M zero bits are padded. The output bits $z_1 z_2 ... z_{BL \log_2 |\mathcal{V}|}$ are periodically interleaved into the sequence $u_1 u_2 ... u_{BL \log_2 |\mathcal{V}|}$ such that

$$u_i = z_{\alpha(i)} \tag{3.10}$$

where

[1] Inequalities (3.8) and (3.9) are also valid for general symbol constellations when R_b is replaced with $R_b / \log_2 |\mathcal{V}|$.

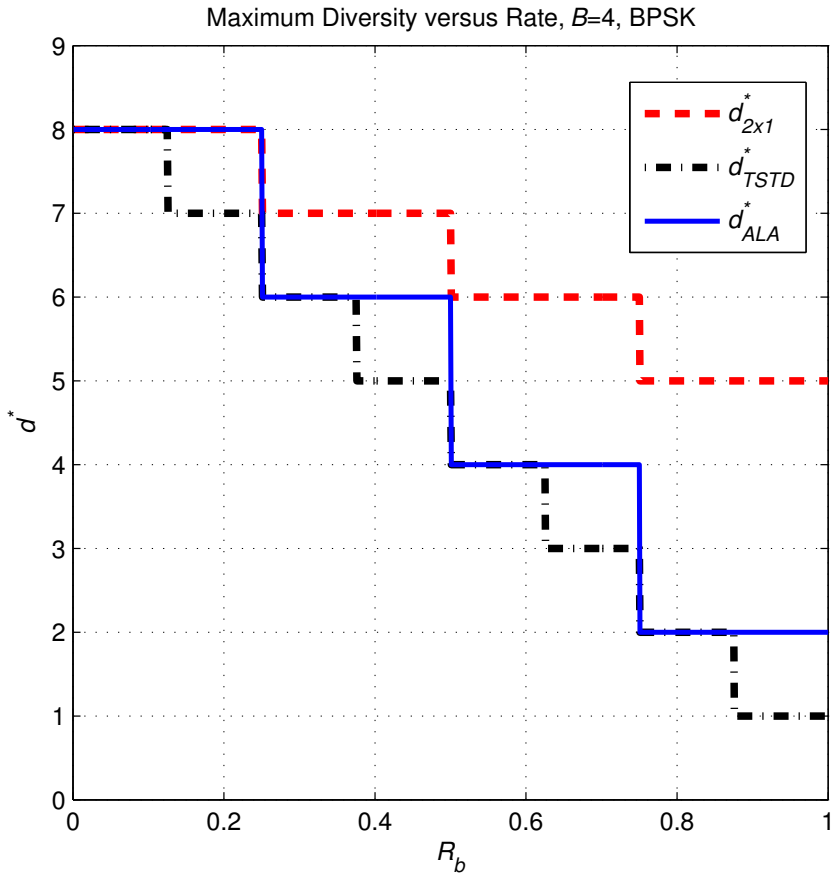

Figure 3.1: Upper bounds for the achievable diversity gains in a 2x1 MISO channel

$$\alpha(i) = 2B \bmod_{L\log_2|\mathcal{V}|/2}(i-1) + \lfloor 2i/L\log_2|\mathcal{V}|\rfloor + 1. \tag{3.11}$$

The block interleaver structure is depicted in Table 3.1. Note that output bits corresponding to the same state transition are transmitted at different channel realizations, when TSTD is used for transmit diversity.

z_1	z_2	z_3	$\cdots$	z_{2B}
z_{2B+1}	z_{2B+2}	z_{2B+3}	$\cdots$	z_{4B}
$\vdots$	$\vdots$	$\vdots$		$\vdots$
$z_{B(L\log_2\|\mathcal{V}\|-2)+1}$	$z_{B(L\log_2\|\mathcal{V}\|-2)+2}$	$z_{B(L\log_2\|\mathcal{V}\|-2)+3}$	$\cdots$	$z_{BL\log_2\|\mathcal{V}\|}$

Table 3.1: The periodic block interleaver

In the next step, consecutive $\log_2|\mathcal{V}|$ interleaved bits are grouped and the sequence $u_1u_2...u_{BL\log_2|\mathcal{V}|}$ are modulated to form $v_1v_2...v_{BL}$ according to the symbol constellation with Gray encoding. Note also that

$$Q = \frac{L\log_2|\mathcal{V}|}{2} - M \tag{3.12}$$

and

$$R_b = \frac{Q}{BL}. \tag{3.13}$$

The symbols $v_1v_2...v_{BL}$ are transmitted according to (3.3) or (3.4), when TSTD or Alamouti scheme is used respectively, and $x_t^b = v_{(b-1)L+t}$. The transmitter end is illustrated in Figure 3.2.

We should point out that not all of the convolutional codes with rate $1/2B$ can achieve full diversity $2B$ in a 2x1 channel with the TSTD technique. Some of the convolutional codes as well as other channel codes that achieve full diversity 2B and the codes that achieve the Singleton bound for SISO BF channels can be found in [27, 26, 25].

Note that d^*_{TSTD} is determined by the minimum block Hamming distance between the code-

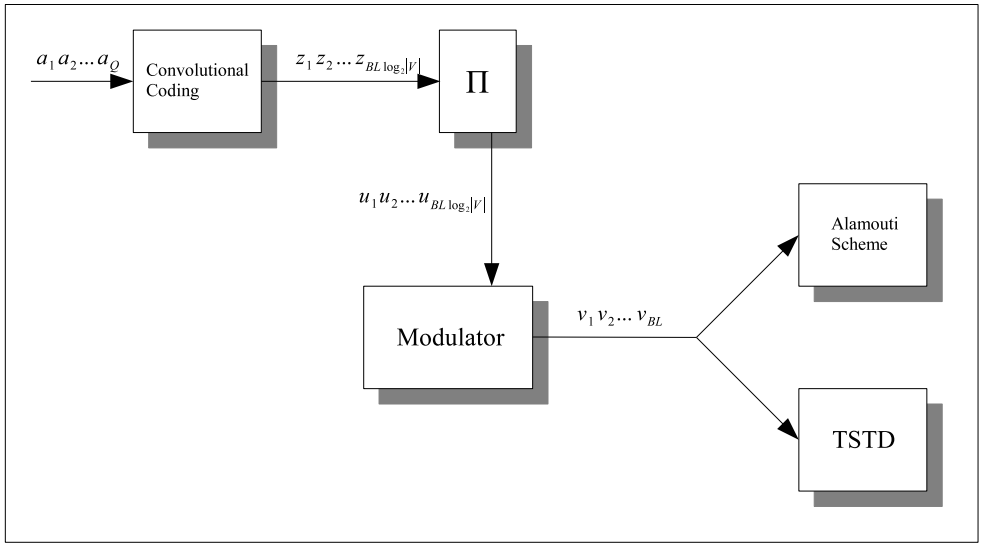

Figure 3.2: Transmitter end for the coherent case

words $D^*_{mbHd,TSTD}$, i.e., the number of block/antenna realizations in which some of the symbols of two codewords differ, in a TSTD system. The minimum block Hamming distance between the codewords of the same outer code over an equivalent Alamouti encoded 2x1 block-fading channel $D^*_{mbHd,ALA}$ is lower bounded by $D^*_{mbHd,ALA} \geq \left\lfloor D^*_{mbHd,TSTD}/2 \right\rfloor$. Note also that the code achieves a diversity gain is of 2x$D^*_{mbHd,ALA}$. Since this is also restricted by the upper bound (3.9), an outer code that achieves the Singleton bound for TSTD (3.8) also achieves the Singleton bound for the Alamouti scheme (3.9).

In [26], some nonconcatenated codes that achieve the Singleton bound in MIMO-BF channel (3.6) are proposed and it is shown that concatenated codes fail to gain the maximum achievable diversity. In [28], the convolutional codes which have a good performance with phase uncertainity in the BF channels are proposed.

3.5 Receiver End

3.5.1 Receiver End for TSTD

As explained in Section 3.4, the groups of $\log_2 |\mathcal{V}|$ bits are modulated into symbols in the constellation $\mathcal{V}$. Suppose that u_i along with $\log_2 |\mathcal{V}| - 1$ adjacent bits are Gray mapped into

$v_{(b-1)L+t}$.

The approximate bit log-likelihood-ratio (LLR), which is introduced in [29], for u_i is extracted from the observed signal y_t^b as

$$\lambda_u(i) = \ln \frac{\max_{v_{(b-1)L+t} \epsilon \mathcal{S}_i} p\left(y_t^b \mid v_{(b-1)L+t}\right)}{\max_{v_{(b-1)L+t} \epsilon \mathcal{S}_i^c} p\left(y_t^b \mid v_{(b-1)L+t}\right)} \tag{3.14}$$

where $\mathcal{S}_i$ is a subset of the symbol constellation $\mathcal{V}$ such that the i'th bit of the inverse Gray mapping of the elements of $\mathcal{S}$ is '0'. For BPSK constellation, the exact LLR for $u_{(b-1)L+t}$ is equivalent to

$$r_{(b-1)L+t} = \begin{cases} \left(h_1^b\right)^* y_t^b & 1 \le t \le L/2 \\ \left(h_2^b\right)^* y_t^b & L/2+1 \le t \le L \end{cases}. \tag{3.15}$$

For PSK constellations,

$$\lambda_u(i) = \min_{v_{(b-1)L+t} \epsilon \mathcal{S}_i} \left| r_{(b-1)L+t} - v_{(b-1)L+t} \right|^2 - \min_{v_{(b-1)L+t} \epsilon \mathcal{S}_i^c} \left| r_{(b-1)L+t} - v_{(b-1)L+t} \right|.^2 \tag{3.16}$$

The approximate LLR's $\lambda_u(i)$ are deinterleaved and $\lambda_z(i)$'s are fed into the Viterbi decoder to find

$$(\hat{a}_1 \hat{a}_2 ... \hat{a}_Q) = \max_{a_1 a_2 ... a_Q} \sum_{i=1}^{BL\log_2|\mathcal{V}|} \xi(z_i)\, \lambda_z(i) \tag{3.17}$$

where

$$\xi(z_i) = \begin{cases} 1 & z_i = 0 \\ -1 & z_i = 1 \end{cases}. \tag{3.18}$$

3.5.2 Receiver End for Alamouti

In the Alamouti scheme, the decisions for the symbols can be obtained by using linear processing. The scaled statistics for $v_{(b-1)L+t}$ and $v_{(b-1)L+t+1}$ are

$$\begin{bmatrix} r_{(b-1)L+t} \\ r_{(b-1)L+t+1} \end{bmatrix} = \begin{bmatrix} h_1^{b*} & h_2^b \\ h_2^{b*} & -h_1^b \end{bmatrix} \begin{bmatrix} y_t^b \\ y_{t+1}^{b*} \end{bmatrix} \tag{3.19}$$

where t is odd.

As in TSTD technique, if BPSK is used (3.38), and if any PSK constellation is used (3.16), holds for the approximate LLR's in the Alamouti receiver.

3.6 Performance Analysis

For a quasi-static or an additive white Gaussian noise (AWGN) channel, the BER performances of the convolutional codes can be easily evaluated with the aid of transfer function, $T(D, N)$. A comprehensive description about tranfer function can be found in [30].

In [31], the transfer function is generalized to be used on a SISO-BF channel with BPSK constellation. Due to the feature of the coding and the interleaver, each output bit corresponding to the same state transition is sent from a different block/antenna realization in the TSTD technique. In the calculation of the generalized transfer function $T(D_{1,1}, D_{2,1}, ..., D_{1,B}, D_{2,B}, N)$ the label of the branches are in the form:

$$\eta = N^{i_0} \prod_{b=1}^{B} D_{1,b}^{i_{1,b}} D_{2,b}^{i_{2,b}}. \tag{3.20}$$

Here the index of D represents the block and the transmit antenna at which the symbol is sent. Since the input bit number in convolutional code that we use is 1 and each output bit is sent from different antennas/blocks, i_0, $i_{1,b}$'s, and $i_{2,b}$'s are either one or zero. An example of the labeling of the branches in a state transition diagram for the convolutional coding with the generator polynomial (5,7) in the octal form, which is used for single block 2x1 MISO channels, is illustrated in Figure 3.3. With an abuse of notation, branch indices b are neglected. In the figure, the solid line indicates that the input bit corresponding to the state transition is '1' and the dotted line indicates that the input bit is '0'.

The transfer function of the example code above is

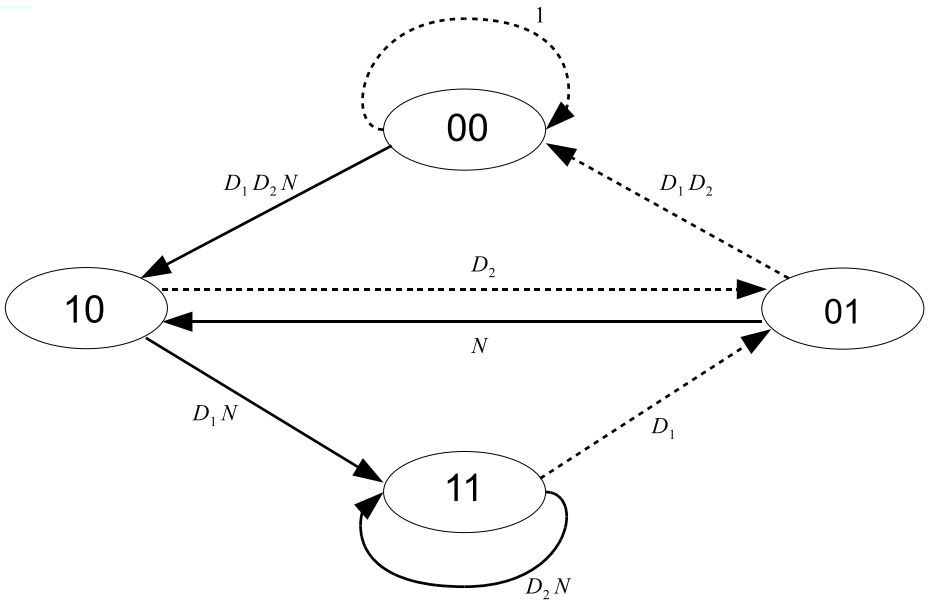

Figure 3.3: The state transition diagram for the (5,7) convolutional code with a periodic interleaver

$$T(D_1, D_2, N) = \frac{-D_1^2 D_2^2 N \left(N D_1^2 - N D_2^2 + D_2\right)}{D_1^2 N^2 - D_2^2 N^2 + 2 D_2 N - 1}. \tag{3.21}$$

In the scenarios that we explained in the previous sections, the BER performance can be found with the aid of the generalized transfer function. When channel gains are fixed, an upper bound for the BER of convolutional code with $T\left(D_{1,1}, D_{2,1}, ..., D_{1,B}, D_{2,B}, N\right)$ and $R = 1/2B$ over a 2x1 MISO-BF channel, collaborated with the TSTD technique, and modulated with BPSK constellation can be found as

$$P_b(h_1^1 h_2^1 ... h_1^B h_2^B) \leq \left. \frac{\partial T\left(D_{1,1}, D_{2,1}, ..., D_{1,B}, D_{2,B}, N\right)}{\partial N} \right|_{N=1, D_{i,b}=e^{-\left|h_i^b\right|^2 \frac{E_s}{N_0}}}. \tag{3.22}$$

Similarly, an upper bound on the BER of the same convolutional code for the Alamouti scheme is found as

$$P_b\left(h_1^1 h_2^1 ... h_1^B h_2^B\right) \leq \left. \frac{\partial T\left(D_{1,1}, D_{2,1}, ..., D_{1,B}, D_{2,B}, N\right)}{\partial N} \right|_{N=1, D_{1,b}=D_{2,b}=e^{-g_b^2 \frac{E_s}{N_0}}} \tag{3.23}$$

where $g_b = \sqrt{(\left|h_1^b\right|^2 + \left|h_2^b\right|^2)/2}$.

It should be take into consideration that the sum of outputs for errorenous paths may not converge to the generalized transfer function for small values of channel gains. Since the region of convergence is complicated and is hard to be found for multidimensional systems [32], we were not able to express the set of channel gains that the upper bound is valid. Moreover, as B increases the generalized transfer function becomes cumbersome to find.

In order to provide the expression of the PER for convolutional codes, we encounter two approaches to be utilized. The first approach is to limit the upper bound for PER before averaging over the channel realizations, which is inefficient in computing due to the need for $2B$ fold integration [33]. In [33], the intantaneous PER is found analytically with the aid of the BER expression. The second one is directly to find the upper bound for average PER values [27]. In the latter approach, however, the upper bound diverges, i.e., results in very high values for small B.

For a fixed channel realization, the PER in TSTD can be upper bounded by [27]

$$PER\left(h_1^1 h_2^1 ... h_1^B h_2^B\right) \leq G_{1,1} - 1 \tag{3.24}$$

where

$$G = A(D_{1,1}, D_{2,1}, ..., D_{1,B}, D_{2,B})^{L/2} \mid_{D_{i,b}=e^{-\left|h_i^b\right|^2 \frac{E_s}{N_0}}} \tag{3.25}$$

and $A\left(D_{1,1}, D_{2,1}, ..., D_{1,B}, D_{2,B}\right)$ is the generalized 2^Mx2^M state transition matrix.

$A_{i,j}(D_{1,1}, D_{2,1}, ..., D_{1,B}, D_{2,B})$ is the entry of $A(D_{1,1}, D_{2,1}, ..., D_{1,B}, D_{2,B})$ at the ith row and jth column and equals the labeling corresponding to the transition from state i to state j.

$G_{1,1} - 1$ corresponds to all the possible paths that start from the all-zero state and end at the all-zero state. To exemplify, for convolutional code with the generator polynomial (5,7) followed by the periodic interleaver, the state transition matrix is

$$A(D_1, D_2) = \begin{bmatrix} 1 & 0 & D_1D_2 & 0 \\ D_1D_2 & 0 & 1 & 0 \\ 0 & D_2 & 0 & D_1 \\ 0 & D_1 & 0 & D_2 \end{bmatrix}. \tag{3.26}$$

Thus, the upper bound for average PER in the TSTD system is found as

$$PER \leq \int_{h_1^1} \int_{h_2^1} \cdots \int_{h_1^B} \int_{h_2^B} \min\left(1, PER(h_1^1 h_2^1 ... h_1^B h_2^B)\right) p\left(h_1^1 h_2^1 ... h_1^B h_2^B\right) dh_1^1 \cdots dh_2^B. \tag{3.27}$$

In order to find the upper bound for PER in the Alamouti scheme, the variables should be modified as

$$D_{1,b} = D_{2,b} = e^{-g_b^2 \frac{E_s}{N_0}}. \tag{3.28}$$

3.7 Outage Probabilities

In [34], it is shown that the random coding bound and the lower bound based on strong converse to the coding theorem are very close to outage probability for block fading channels with large L, and even with moderate L values. Motivated by this result, we compare outage probabilities of two systems to investigate the limits of these two systems for BPSK constellation.

For convenience will give two definitions:

$$y' = \sqrt{\gamma \left|h_i^b\right|^2} x + n' \tag{3.29}$$

$$y'' = \sqrt{\gamma g_b^2} x + n'' \tag{3.30}$$

where n' and n'' are ZMCSCG noise samples with unit power.

The outage probability for TSTD technique in a 2x1 MISO-BF with B blocks P_{out}^{TSTD} equals $Pr\left(R_b > I_{TSTD}\left(h_1^1 h_2^1 ... h_1^B h_2^B, \gamma\right)\right)$ where

$$I_{TSTD}\left(h_1^1 h_2^1 ... h_1^B h_2^B, \gamma\right) = \frac{1}{2B} \sum_{b=1}^{B} \sum_{i=1}^{2} \int_{y'} \left[\sum_{x} q(x) p(y'|x, h_i^b) \log_2 \frac{p(y|s, h_i^b)}{p(y|h_i^b)} \right] dy \tag{3.31}$$

is the average mutual information, $x = \pm 1$; and the probability of x is $q(x) = 1/2$ for all x.

For the Alamouti scheme, the outage probability P_{out}^{ALA} is defined similarly with

$$I_{ALA}\left(h_1^1 h_2^1 ... h_1^B h_2^B, \gamma\right) = \frac{1}{B} \sum_{b=1}^{B} \int_{y''} \left[\sum_{x} q(x) p(y|s, g_b) \log_2 \frac{p(y|s, g_b)}{p(y|g_b)} \right] dy. \tag{3.32}$$

3.8 Numerical Results for Coherent Channels

With the BPSK constellation, we compare the error performances and the outage probabilities for the TSTD technique and the Alamouti scheme with the aid of Monte Carlo simulations and the analytical results given in Sections 3.6 and 3.7. Obtained after using the encoding and decoding structures explained in the previous sections, the results are depicted in Figures 3.4, 3.5, and 3.6 for $B = 1, 2$, and 3, respectively. We fix the block length as $L = 100$. The convolutional codes are borrowed from [25] and the generator polynomials are given in octal form. In the simulation minimum 400 erroneous packets are collected.

It can be seen in Figure 3.4 that the PER's of the two systems are close to each other with the Alamouti scheme having roughly 1dB better performance. As the outage probabilities for the two transmit diversity schemes are close to each other, the discrepancy between the PER's are smaller if $B = 2$ or 3 as depicted in Figures 3.5 and 3.6. The closeness of the performances of the systems is also accompanied by the closeness of the outage probabilities on the same order. The differences between the analytic upper-bounds for the PER's and the simulation results for the PER's are nearly 2 dB. Note that full spatio-temporal diversity $2B$ is achieved in all cases.

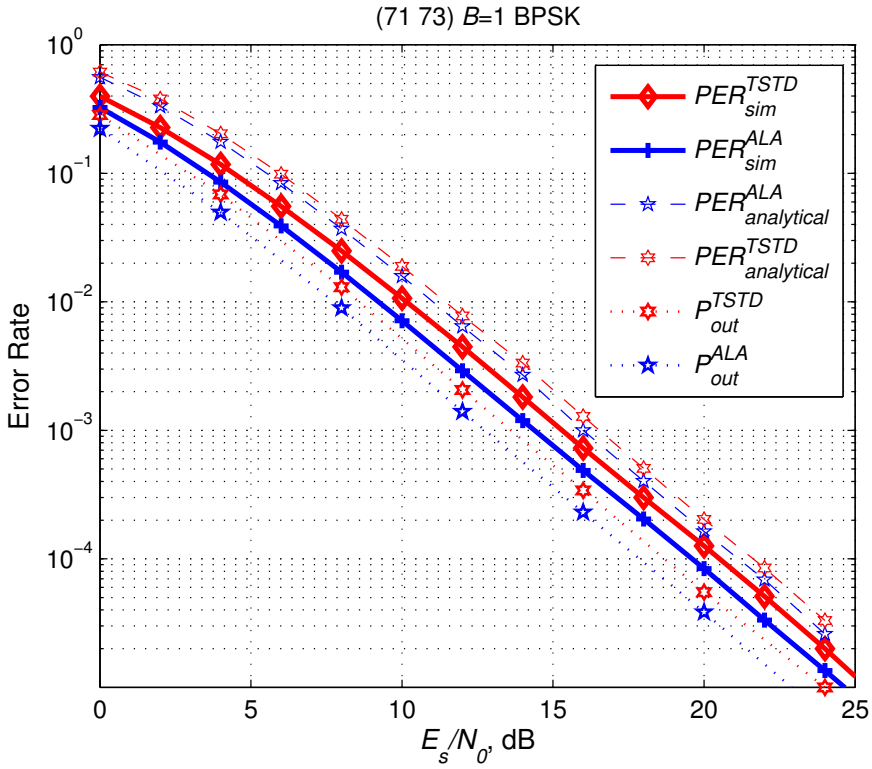

Figure 3.4: Simulation of convolutional code with generator polynomial (71 73), B=1, R_b=0.45

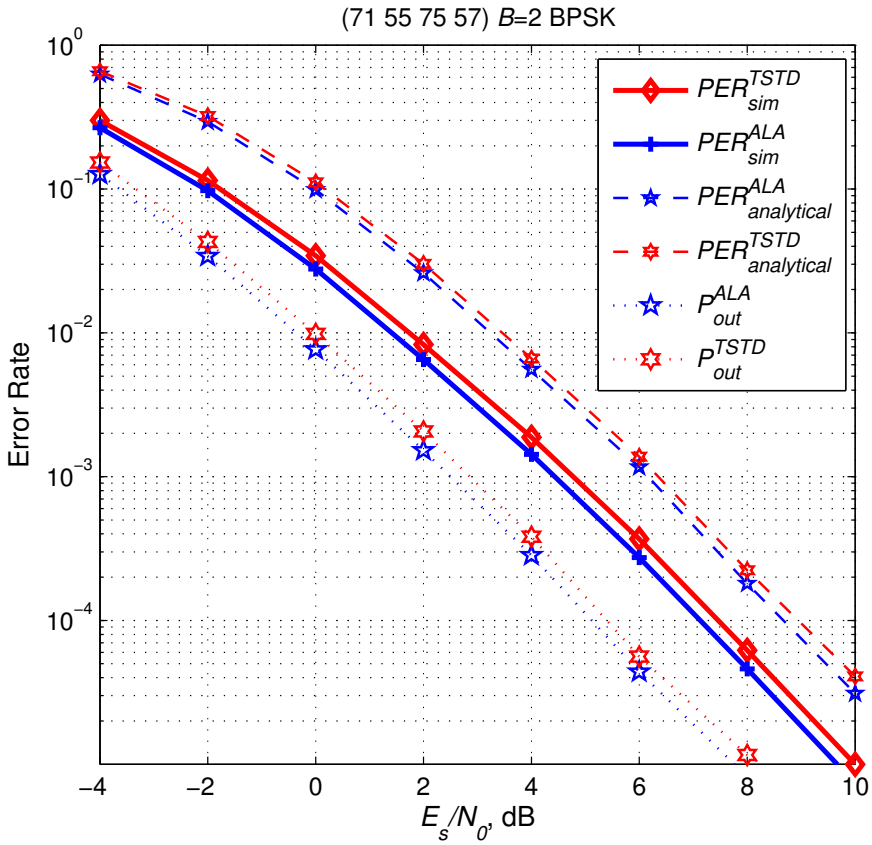

Figure 3.5: Simulation of convolutional code with generator polynomial (71 55 75 57), $B = 2$, $R_b = 0.225$

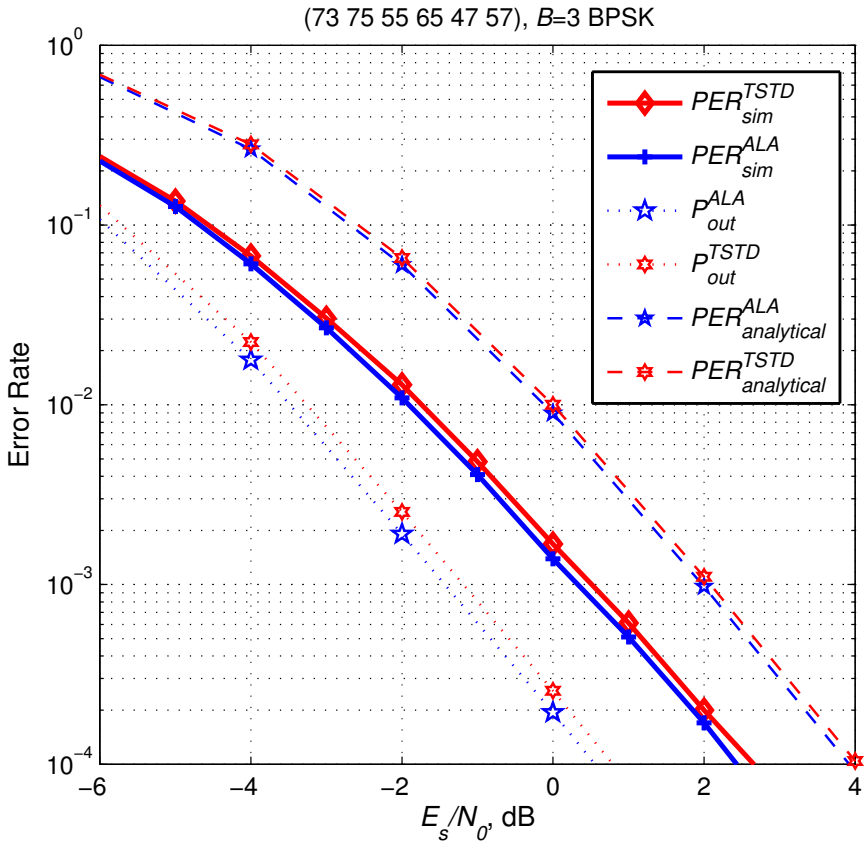

Figure 3.6: Simulation of convolutional code with generator polynomial (73 75 55 65 47 57), $B = 3$, $R_b = 0.15$

3.9 Noncoherent Block-Fading MISO Channels

So far in this chapter we assumed that the CSI is perfectly available at the receiver and compared the TSTD and the Alamouti scheme under this assumption. In this section, we carry out a similar comparison, including simulation results, when the CSI is available neither at the transmitter nor at the receiver side. A suitable differential encoding/detection is used for each system and no attempt is done in order to estimate the CSI.

We consider a 2x1 MISO-BF channel where the the transmit diversity techniques are concatenated with the rate-$1/2B$ convolutional codes. In order to use the differential method, $2B$ known symbols are inserted in both systems. The number of symbols in each block is assumed to be $L + 2$, where the extra two symbols are used as reference. The bit rate in the noncoherent channel is

$$R_b = \frac{Q}{B\,(L+2)}.$$

3.9.1 TSTD

After Q input bits are encoded and interleaved as explained in Section 3.4, differential phase-shift keying (DPSK) is used for transmission. A known symbol is put just after each antenna switch such that

$$x_1^b = x_{L/2+1}^b = 1. \tag{3.33}$$

Representing $v_{(b-1)L+t}$ as the PSK modulated symbols, the transmitted signals are differentially encoded as

$$x_{t+1}^b = \begin{cases} x_t^b v_{(b-1)L+t} & 1 \le t \le L/2 \\ x_t^b v_{(b-1)L+t-1} & L/2+1 \le t \le L+1 \end{cases}. \tag{3.34}$$

The statistics are found by differentially decoding as

$$r_{(b-1)L+t} = \begin{cases} y^b_{t+1} y^{b*}_t & 1 \le t \le L/2 \\ y^b_{t+2} y^{b*}_{t+1} & L/2+1 \le t \le L \end{cases} . \tag{3.35}$$

Ignoring the cross-interference noise, the approximate LLR's are found using (3.16) and are given to the Viterbi decoder.

3.9.2 Differential Alamouti Scheme

When the CSI is not available, differential counterpart of the Alamouti scheme, differential STBC for $N_t = 2$ is used.

The encoded and modulated symbols $v_{(b-1)L+t}$ are mapped into the (A, B) pairs as in (2.38). Two known symbols are inserted at the beginning of each block:

$$x^b_1 = x^b_2 = 1. \tag{3.36}$$

The differential encoding is done via

$$\begin{bmatrix} x^b_t \\ x^b_{t+1} \end{bmatrix} = A \begin{bmatrix} x^b_t \\ x^b_{t+1} \end{bmatrix} + B \begin{bmatrix} x^b_t \\ x^b_{t+1} \end{bmatrix}. \tag{3.37}$$

where t is odd. As explained in Section 2.5 the statistics for A and B are

$$\begin{aligned} R_A &= y^{b*}_{t-2} y_t + y^b_{t-1} y^{b*}_{t+1} \\ R_B &= -y^{b*}_{t-1} y^b_t + y^b_{t-2} y^{b*}_{t+1} \end{aligned} . \tag{3.38}$$

The statistics for $v_{(b-1)L+t}$ and $v_{(b-1)L+t+1}$ are

$$r_{(b-1)L+t} = A + B^*, r_{(b-1)L+t+1} = B^* - A \tag{3.39}$$

Ignoring the cross-interference noise, the approximate LLR's are found using (3.16) and are given to the Viterbi decoder.

The transmitters are illustrated in Figure 3.7.

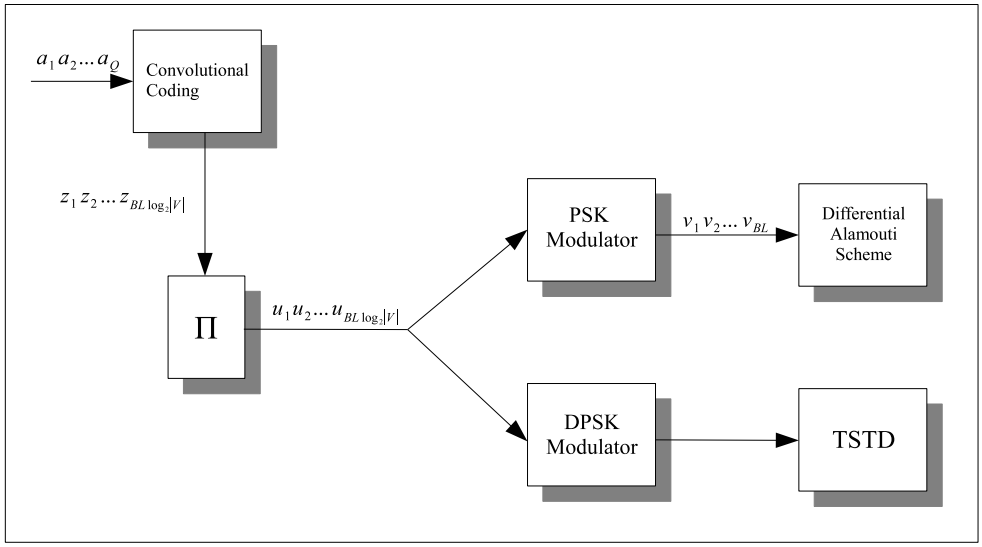

Figure 3.7: Transmitter End for Differential Encoding

3.9.3 Numerical Results

Like the coherent case, we use BPSK as the constellation and the encoding/interleaver explained before. The memory order of the convolutional code is $M = 3$. The simulation results for $B = 1$, 2, and 3 are depicted in Figures 3.8, 3.9, and 3.10 respectively. In Figure 3.8 it is seen that the error performances are close to each other. DSTBC have roughly 1 dB better PER performance. Supporting the results in the coherent case, the discrepancy between the error performances of the TSTD and DSTBC is smaller with $B = 2,3$. Note that the systems achieve full diversity $1/2B$ for all B values.

Using the analytical and simulation results, it is shown that the performances of the coherent Alamouti scheme and coherent TSTD are close to each other in the previous section. In this section the closeness between the performances of DSTBC, the differential counterpart of the coherent STBC, and TSTD with DPSK is verified.

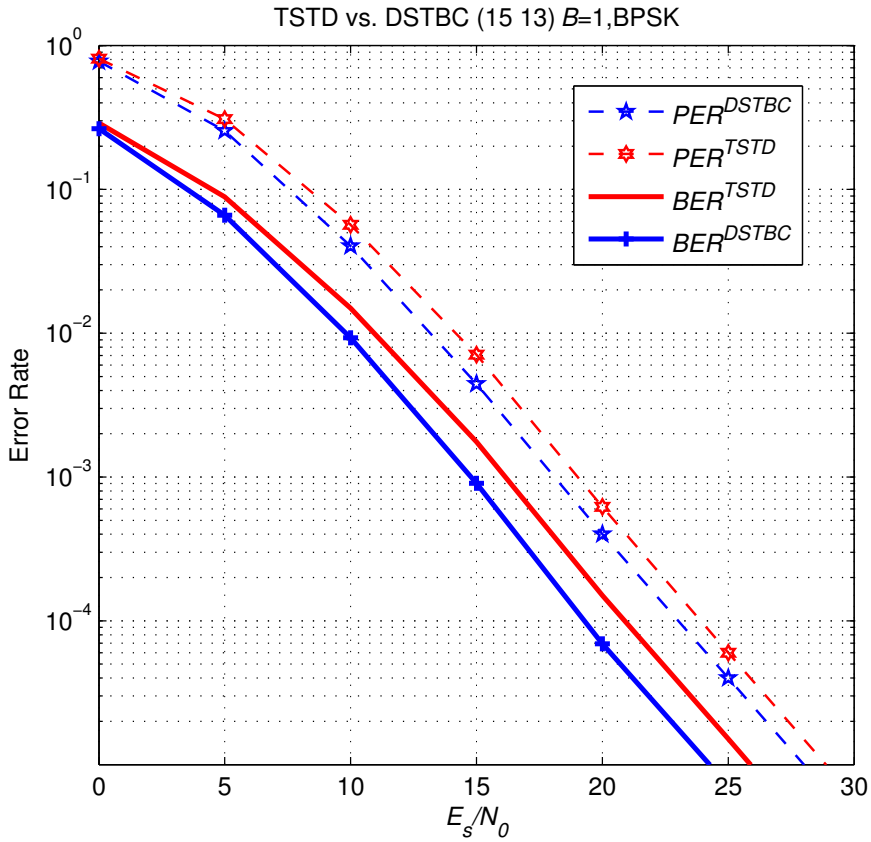

Figure 3.8: Simulation of convolutional code with g: (15 13), $B = 1$

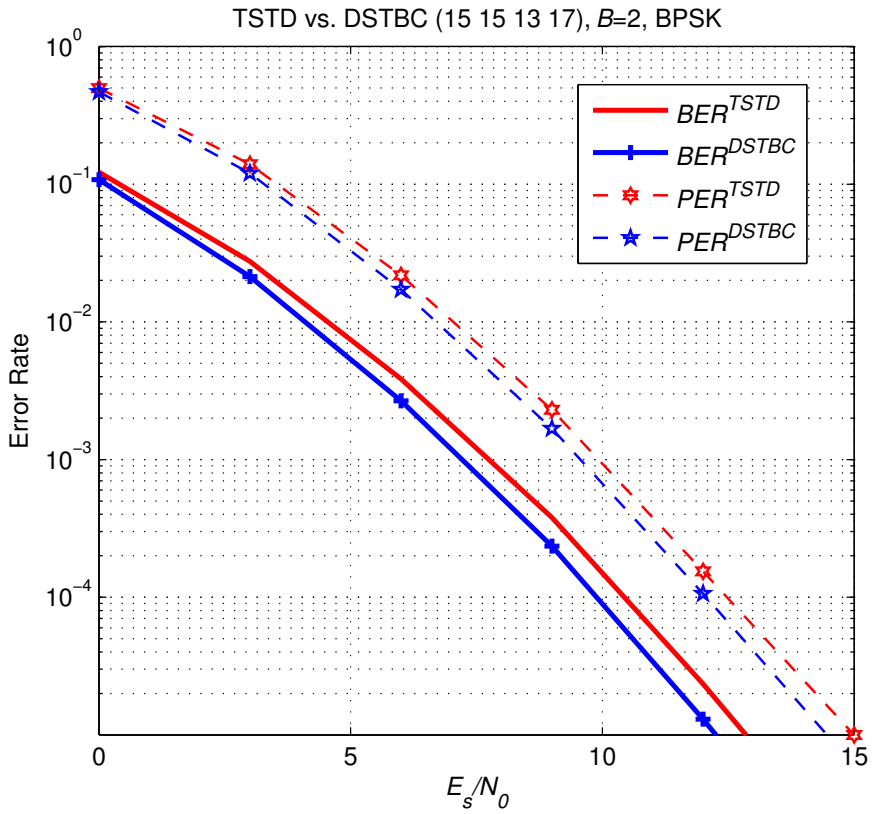

Figure 3.9: Simulation of convolutional code with g: (15 15 13 17), $B = 2$

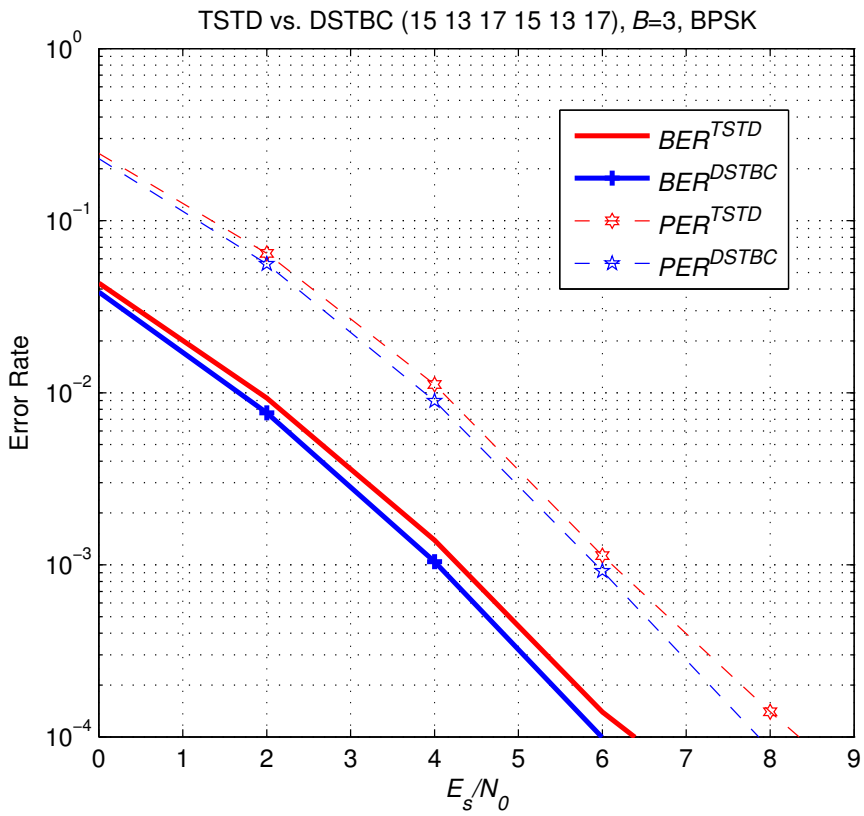

Figure 3.10: Simulation of convolutional code with g: (15 13 17 15 13 17), $B = 3$

CHAPTER 4

STBC PERFORMANCE IN TIME-VARYING CHANNELS

This chapter is devoted to the analyses of the performance degradation of STBC's due to the channel coefficients variation in time and imperfections in the channel estimates. In contrast to the scenario in Chapter 3, we do not utilize channel codes concatenated with the STBC's. A channel estimation technique for time-varying flat-fading channels and uncoded symbol error performance in Rayleigh distributed continuous time-varying MISO channel with channel uncertainty are given. The effect of time-variation on the symbol error performance of the differential STBC's is also discussed.

4.1 PSAM

Pilot Symbol Assisted Modulation (PSAM) is a method for channel estimation in flat-fading channels and is particularly suitable for rapidly fading channels [35]. Instead of sending the training sequences at the beginning of transmission, known pilot symbols are inserted between the data symbols and the channel coefficients are estimated by the aid of transversal Wiener filters, which are optimal in the minimum mean square error (MMSE) sense by definition. In order to estimate the channel gain coefficient at a particular time t, K nearest pilot symbols are used for estimation. The pilot symbols are inserted equally spaced with a pilot spacing F. The placement of inserted pilot symbols in a SISO continuous time-varying fading channel is illustrated in Figure 4.1, where the solid vertical lines represent the pilot symbols and the dotted lines represent the data symbols. The channel response to the pilot symbol at t is perturbed by a ZMCSCG noise sample n_t with variance N_0. Without loss of generality, we will assume that K is even.

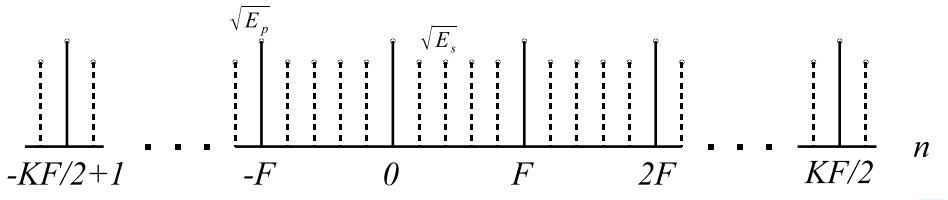

Figure 4.1: Placement of the pilot symbols among the data symbols during the transmission

For the estimation of the channel coefficient h_t in a SISO flat-fading channel at time t, the interpolator vector (Wiener filter) is given as

$$\mathbf{p}_t = \begin{bmatrix} p_{t,-K/2+1} \\ \vdots \\ p_{t,0} \\ p_{t,1} \\ \vdots \\ p_{t,K/2} \end{bmatrix} \tag{4.1}$$

where

$$p_{t,l} = \sqrt{E_p} h_{(\lfloor t/F \rfloor + l)F} + n_{(\lfloor t/F \rfloor + l)F} \tag{4.2}$$

and E_p is the pilot symbol energy. The autocorrelation function of $\mathbf{p}_t$ is defined as

$$\mathcal{E}\left\{\mathbf{p}_t \mathbf{p}_t^H\right\} = \mathbf{R}_p = \begin{bmatrix} r_{0,0} & r_{0,1} & \cdots & r_{0,K-1} \\ r_{1,0} & r_{1,1} & \cdots & r_{1,K-1} \\ \vdots & \vdots & \ddots & \vdots \\ r_{K-1,0} & r_{K-1,1} & \cdots & r_{K-1,K-1} \end{bmatrix}. \tag{4.3}$$

For a flat-fading channel with the Jakes' spectrum [36] having a maximum Doppler frequency f_d, the entries of $\mathbf{R}_p$ becomes

$$r_{i,j} = E_p J_0 \left(2\pi f_{dn} \left(i - j\right) F\right) + N_0 \delta_{i,j}. \tag{4.4}$$

where $f_{dn} = f_d T_s$, T_s is symbol duration and $\delta_{i,j}$ is the Kronecker delta function.

The cross-correlation vector is

$$\mathcal{E}\{\mathbf{p}_t h_t^*\} = \mathbf{c}_t = \begin{bmatrix} c_{-K/2+1} \\ \vdots \\ c_0 \\ c_1 \\ \vdots \\ c_{K/2} \end{bmatrix} \tag{4.5}$$

where

$$c_i = \sqrt{E_p} J_0 \left(2\pi f_{dn} |iF - t|\right) \tag{4.6}$$

again for fading channels with the Jakes' spectrum. The Wiener filter coefficients are then given as the vector

$$\mathbf{w}_t = \mathbf{R}_p^{-1} \mathbf{c}_t. \tag{4.7}$$

The estimation of the flat-fading channel coefficient at time t is

$$\hat{h}_t = \mathbf{w}_t^H \mathbf{p}_t. \tag{4.8}$$

Note that $\mathbf{w}_{t_1} = \mathbf{w}_{t_2}$ for $\mathrm{mod}_F |t_1 - t_2| = 0$ and $\mathbf{p}_{t_1} = \mathbf{p}_{t_2}$ for $\lfloor |t_1 - t_2| / F \rfloor = 0$.

In order to reconstruct the channel gain coefficients of a fading channel with a band-limited spectrum, the pilot symbols should sample the process with an adequate frequency. In order for the pilot responses not to have an unaliased spectrum, the pilot spacing in a fading channel with Jakes' spectrum must satisfy the Nyquist criterion:

$$F \leq \frac{1}{2 f_{dn}}. \tag{4.9}$$

Assume for the moment that K is infinite. In this case for the continuous flat-fading channels with a band-limited power spectrum density (PSD) of fading coefficient, the MMSE is [37, 38]

$$\mathcal{E}\left\{\left|h_t - \hat{h}_t\right|^2\right\} = \xi_{min} = 1 - \int_{-B_f}^{B_f} \frac{\gamma_p S_h^2(v)}{F + \gamma_p S_h(v)} dv \tag{4.10}$$

where $S_h(v)$ is the PSD of h_t, B_f is the positive bandwidth, and γ_p denotes E_p/N_0. For a fading channel with the Jakes' spectrum, the MMSE is [39]

$$\xi_{min} = 1 - \frac{\operatorname{arctanh}\sqrt{1 - \left(\frac{\gamma_p}{F\pi f_{dn}}\right)^2}}{\frac{\pi}{2}\sqrt{\left(\frac{F\pi f_{dn}}{\gamma_p}\right)^2 - 1}}. \tag{4.11}$$

Note for infinite K that ξ_{min} does not depend on the position (time index) of the estimated channel coefficient with respect to the pilots, i.e., ξ_{min} corresponding to the channel gain coefficient at the middle of two pilot symbols and the channel gain coefficient adjacent to a pilot symbol are the same. For a finite but sufficiently large K, the dependence of ξ_{min} on the position is still not significant. For example in a PSAM scheme with $K = 36$, $F = 12$, and $f_{dn} = 0.01$, the variation is less than 0.1% [40]. Provided that (4.9) holds and K is infinite, ξ_{min} goes to zero as γ_p goes to infinity.

In our scenarios we will generalize PSAM for a 2x1 system as follows. While the first transmit antenna sends a pilot symbol, the second antenna remains silent, and visa versa at the following time slot. Whilst the pilot symbols are sent during two symbol durations, data symbols are transmitted during adjacent $F - 2$ symbol durations. Since there is no inter-transmit-antenna-interference (ITAI), previous results for SISO channel hold.

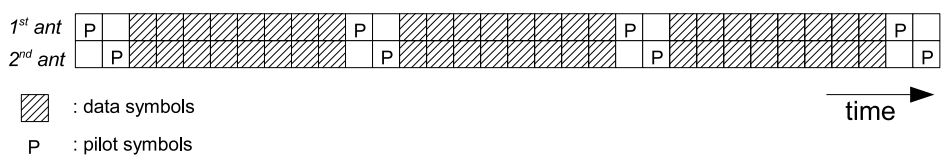

Figure 4.2: Pilot Insertion for two transmit antennas

4.2 Performance of the Alamouti Scheme With Channel Uncertainty

Due to the limited pilot energy the channel gain coefficients cannot be estimated perfectly with the PSAM technique. The channel estimation error leads to performance degradation and induces an error floor, i.e., that even if the SNR increases the error performance becomes bounded. Note that the estimation error is orthogonal to the channel estimate and the variance of any channel estimate is smaller than the variance of the corresponding channel gain coefficient, which equals one.

Let us assume that the channel gain coefficients in a 2xN_r quasi-static Rayleigh fading channel with unit power gain are estimated with the aid of pilot symbols having the same energy for both antennas. As in (2.32), the symbols that are encoded with the Alamouti scheme before transmission are detected with linear processing using the estimated channel gain coefficients as if they are perfect. The performance degradation due to the channel uncertainty is given analytically in [41]. Using the Alamouti scheme and linear processing at the receiver, the BER with BPSK modulation on a quasi-static Rayleigh fading channel can then be given as

$$P_b = \frac{1}{4}\left(1 - \sqrt{\frac{A}{2+A}}\right)^2 \left(2 + \sqrt{\frac{A}{2+A}}\right) \tag{4.12}$$

where

$$A = \frac{E_s\left(1-\sigma_e^2\right)}{N_0 + E_s\sigma_e^2}, \tag{4.13}$$

σ_e^2 is the channel estimation error variance and N_r is one. It can also be generalized to the multiple receive antenna case as [36]

$$P_b = \left(1 - \sqrt{\frac{A}{2+A}}\right)^{2N_r} \sum_{c=0}^{2N_r} 2^{-2N_r-c} \begin{pmatrix} 2N_r + c - 1 \\ c \end{pmatrix} \left(1 + \sqrt{\frac{A}{2+A}}\right)^c. \tag{4.14}$$

Figure 4.3 illustrates the performance degradation due to the channel uncertainty in a 2x1 quasi-static Rayleigh fading channel with unit energy. The channel gains are uncorrelated with respect to the transmit antennas. With a channel estimation error of $\sigma_e^2 = 0.01$ the error floor is at 7.4x10^{-5}, whereas the error floor is at 1.6x10^{-3} if $\sigma_e^2 = 0.05$.

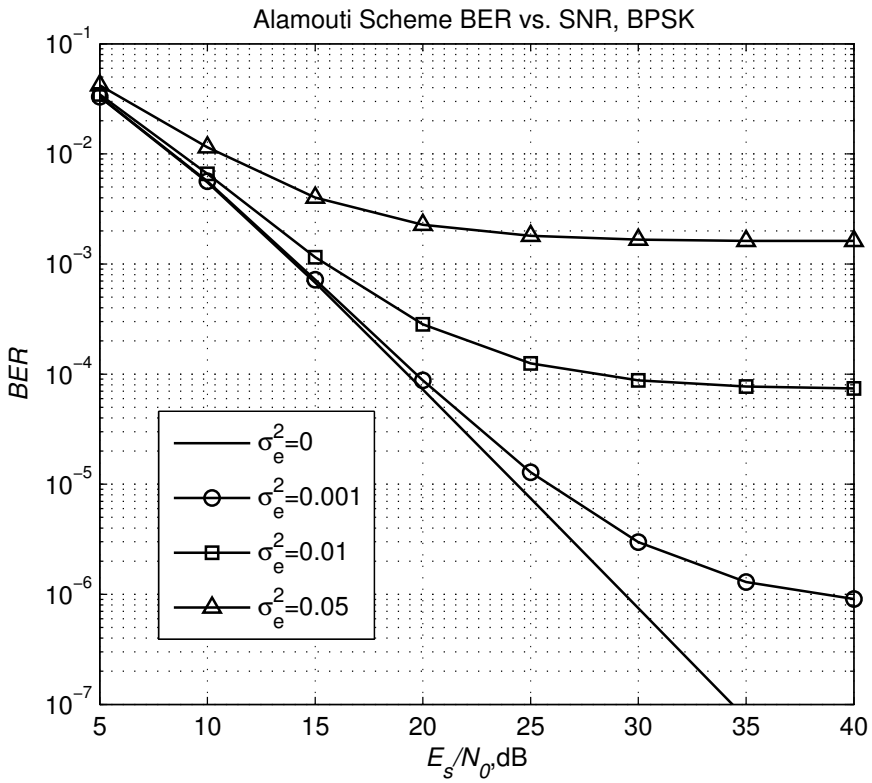

Figure 4.3: The effect of the channel estimation error on the error performance of the Alamouti scheme with BPSK modulation. (N_t=2, N_r=1).

4.3 Performance of the Alamouti Scheme Over Time-Varying Channels

The linear processing operation in (2.32) presumes that the channel gain coefficients do not change within two symbol durations. Considering (2.30), Θ in (2.31) for a time-selective 2x1 MISO channel is modified as

$$\Theta = \begin{bmatrix} h_t^1 & h_t^2 \\ h_{t+1}^{2*} & -h_{t+1}^{1*} \end{bmatrix} \tag{4.15}$$

where h_t^1 and h_t^2 denote the channel gain coefficients of the first and the second antennas at time t respectively. Since $\Theta^H\Theta$ is non-diagonal, ITAI occurs, even if the channel coefficients are perfectly known. Therefore, the linear processing renders the Alamouti scheme susceptible to time-variation of channel coefficients.

Consider the Alamouti scheme over a 2x1 Rayleigh, equally and independently distributed flat-fading channel with BPSK constellation. The average BER when the correlation coefficients between adjacent channel gain coefficients are the same for h_t^1 and h_t^2 is [42]

$$P_b = \frac{1}{4}\left(1 - \Upsilon\right)^2 \left(2 + \Upsilon\right) \tag{4.16}$$

where

$$\Upsilon = \sqrt{2 + 2N_0 - \rho^2} \tag{4.17}$$

and ρ is the correlation coefficient between adjacent channel gain coefficients in time for both h_t^1 and h_t^2. If the Doppler power spectrum of h_t^1 (and h_t^2) is Jakes' spectrum,

$$\rho = J_0\left(2\pi f_{dn}\right). \tag{4.18}$$

Along with linear processing, several alternative receiver structures for the Alamouti encoded systems without any outer channel code have been proposed. In [43], receivers based on zero-forcing and decision feedback have been investigated. In [44], a quasi-ML decoder

is suggested. Another receive structure based on interference cancellation is given in [40]. However these receiver structures are not in the scope of our study.

4.4 Performance of the Alamouti Scheme Over Time-Varying Channels with PSAM

In the Alamouti encoded systems where the channel gain coefficients are estimated with PSAM, the combined detrimental effects of the channel estimation error and the time-variation on the error performance must be investigated. The BER of the BPSK modulated Alamouti scheme in a 2x1 Rayleigh time-selective fading channel is found with the aid of (4.16) where Υ is modified as [42]

$$\Upsilon = \left(\frac{4\left(1+\gamma_s^{-1}\right)}{\varepsilon_0} - \left(\frac{\varepsilon_1}{\varepsilon_0}\right)^2 \right)^{-1/2} \tag{4.19}$$

in which

$$\begin{aligned} \varepsilon_0 &= 2\psi_0^H \left(\Psi_0 + \gamma_p^{-1}\mathrm{I}_K\right)^{-1} \psi_0 \\ \varepsilon_1 &= 2\psi_1^H \left(\Psi_0 + \gamma_p^{-1}\mathrm{I}_K\right)^{-1} \psi_0 \end{aligned} . \tag{4.20}$$

The parameters ψ_0, ψ_1, and Ψ_e $(e = 0, 1)$ are defined as follows. The entry at the mth row and nth column of Ψ_e equals $\mathcal{E}\left\{h_{t+e+m}^{1,2} h_{t+n}^{1,2*}\right\}$ and ψ_e is the $K/2+1$th column of Ψ_e. Since the channel estimation error will diminish as SNR increases provided that $E_p = \beta E_s$, K is sufficiently large and (4.9) holds, it can be inferred that only the variation of channel gain coefficients in time degrades the performance at high SNR.

4.5 Optimum Pilot Spacing

In Sections 4.2 and 4.4, it is revealed that noisy channel estimates lead to degradation in error performance. Considering (4.10), it can be deduced that either F should be decreased or E_p should be increased. However, both approaches leave a reduced energy for the data symbols. Thus, there is a trade-off between better channel estimation and increased E_s. The optimization can be performed in different manners. Either F with constant E_p or E_p with

constant F can be optimized. The parameters can be optimized jointly as well. Besides, the parameters can be optimized with respect to the error performance or the optimization can be done in the information-theoretic sense.

The maximization of the uncoded symbol error performance of the Alamouti encoded systems with respect to F is analyzed in [40]. The channel gain coefficients of the 2x1 Rayleigh channel that belong to the first and second transmit antennas are independent and have the Jakes' spectrum with the same f_{dn}. The symbols are modulated M-ary PSK constellation. It is also assumed that and $E_s = \frac{F-2}{F} E_b \log_2 M$ and $E_p = E_s$. The optimum pilot spacing is given as [40]

$$F_{opt} = 2\left\lfloor 1 + \sqrt{1 + \frac{1}{4 f_{dn}}} \right\rfloor. \tag{4.21}$$

Note that F_{opt} does not depend on SNR.

4.6 DSTBC Over Time-Varying Channels

In the conventional DPSK modulated systems, each symbol is detected using two-symbol observations without the need of CSI. The error performance deteriorates and an error floor is induced if the flat-fading channel is not constant within two symbol durations. Average BER for differential BPSK modulation in Rayleigh SISO fading channels with time-variation is given as [36]

$$P_b = \frac{1}{2}\left(\frac{1 + \gamma_s (1 - \rho)}{1 + \gamma_s}\right). \tag{4.22}$$

In the fading channels with Jakes' spectrum the error floor is also approximately given as [36]

$$P_{b,floor} \approx 0.5 \left(\pi f_{dn}\right)^2. \tag{4.23}$$

In the DSTBC systems, details of which are given in Section 2.5, it is assumed the channel gain coefficients are constant within 4 symbol durations. Like the DPSK modulated systems,

the DSTBC is also susceptible to time-variation. The average BER of the BPSK modulated DSTBC over 2x1 Rayleigh time-varying channel is as [45]

$$P_b = \frac{1}{4}(1-\mu)^2(2+\mu) \tag{4.24}$$

where

$$\mu = 1/\sqrt{1+2\left[\left(\frac{\gamma_s+1}{\gamma_s\rho[1]}\right)^2 - 1\right]}. \tag{4.25}$$

Actually in the derivation [45], it is assumed that channel gain coefficients are constant within 2 symbol durations and then change with the autocorrelation function of the channel. The autocorrelation function $\rho[1]$ is modified as

$$\rho[1] = \frac{1}{3}\sum_{i=1}^{3}\rho(i) \tag{4.26}$$

where

$$\rho(i) = J_0(2\pi f_{dn} i) \tag{4.27}$$

in order to generalize (4.24) to the symbol-to-symbol time-varying channels with Jakes' spectrum.

Note that $E_s = E_b \log_2 M$ as opposed to the Alamouti scheme with PSAM. The generalizations of the analytic symbol error rate evaluation to other PSK constellations are also given in [45].

4.7 Numerical Results

In this section we present the simulation results of the performance of the Alamouti scheme with PSAM and DSTBC over 2x1 Rayleigh flat-fading channels. The time-varying channel gain coefficients with Jakes' spectrum are independent in space, and f_{dn} for the first and the second antenna are the same. There is no concatenated coding and BPSK is used as symbol constellation. For the Alamouti scheme, F is optimized as in (4.21) and it is fixed that

$E_p = E_s$. For different f_{dn} values, the simulation results are accompanied with the analytical performance results in (4.16) and (4.24).

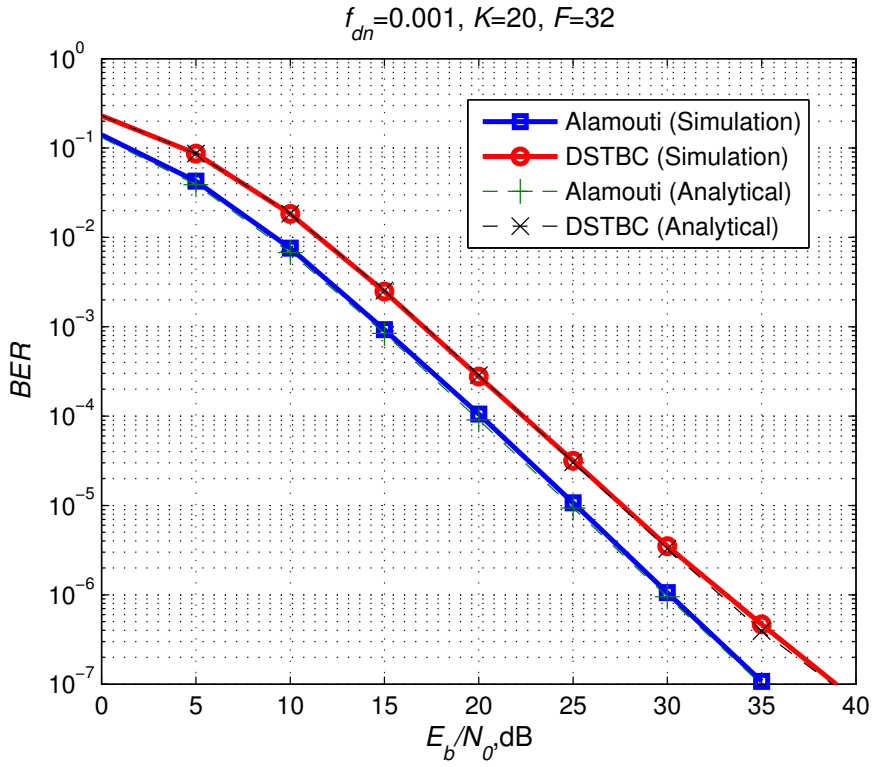

Figure 4.4: Performance of the coherent and noncoherent STBC's with the BPSK modulation with Jakes' model, $f_{dn} = 0.001$.

In Figure 4.4, the average BER values versus E_b/N_0 for $f_{dn} = 0.001$ are shown. Note that full-diversity, which is 2, is achieved with both systems. DSTBC has 2.7 dB loss from the Alamouti scheme. If the overhead energy is taken into account, the plots are consistent with Figure 2.5. The simulation results are well matched to the analytical results. The performances are not affected by the time-variation and the error floors are not observable at this f_{dn} value. Figure 4.5 depicts the performance results for $f_{dn} = 0.01$. This maximum Doppler spread corresponds to a mobile system operating at 900 MHz with 9.6 kbauds and with a speed of approximately 110 km/h [40]. While the error floor for the Alamouti scheme is $8.3\text{x}10^{-7}$, the error floor for DSTBC is $5.4\text{x}10^{-5}$. In Figure 4.6, it is shown that the error floor are very high if $f_{dn} = 0.03$. It corresponds to the 1.9 GHz personal communications services (PCS) system, with 6.4 kbaud symbol rate and at 110 km/h [40]. The error floor starts at nearly 40dB for the Alamouti scheme and nearly 30 dB for DSTBC.

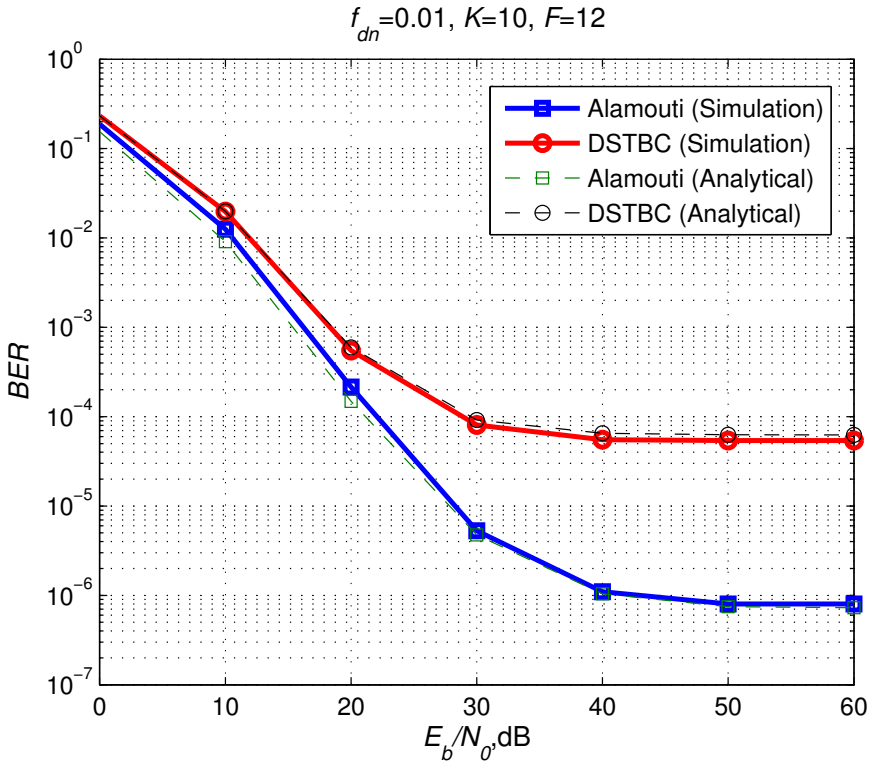

Figure 4.5: Performance of the coherent and noncoherent STBC's with the BPSK modulation with Jakes' model, $f_{dn} = 0.01$.

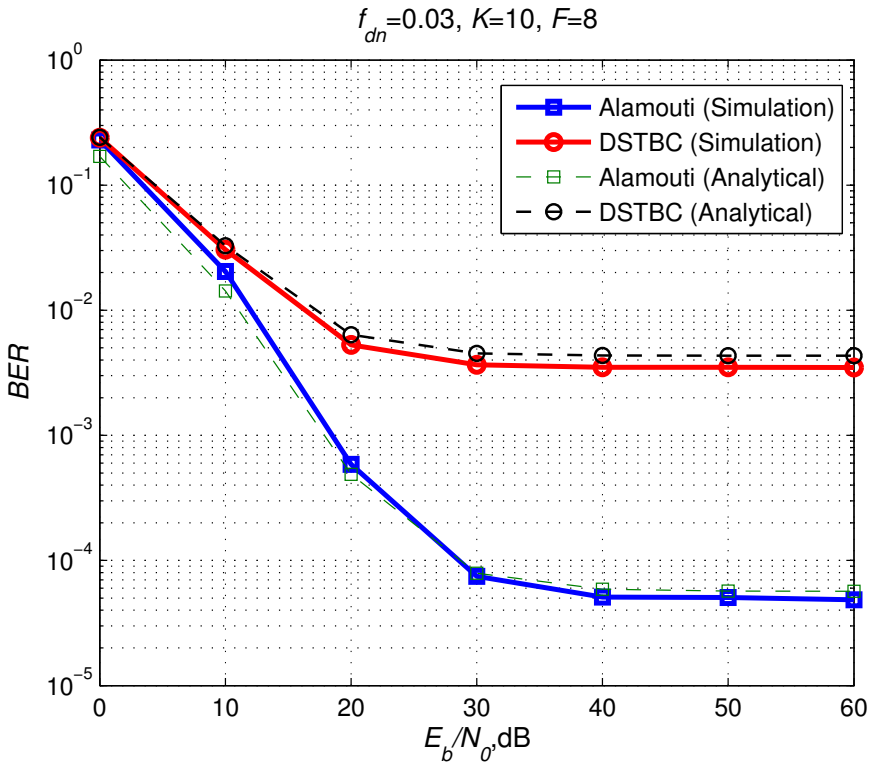

Figure 4.6: Performance of the coherent and noncoherent STBC's with the BPSK modulation with Jakes' model, $f_{dn} = 0.03$.

Since larger K values lead to increased complexity, the dependence of the performance of the Alamouti scheme on K is important. In Figure 4.7, the performance results for the Alamouti scheme with PSAM is given for $f_{dn} = 0.03$ with different K values. For the optimum F value of 8, increasing K to more than 4 does not provide a significant improvement in the BER performance. For larger values of f_{dn}, the channel coherence time is smaller. Since the correlation between the channel gain coefficient to be detected and the pilot symbols at the beginning and the end of the interpolator vector in (4.1) are gets smaller as f_{dn} increases, it can be inferred that as as the sufficient K increases with increasing f_{dn}.

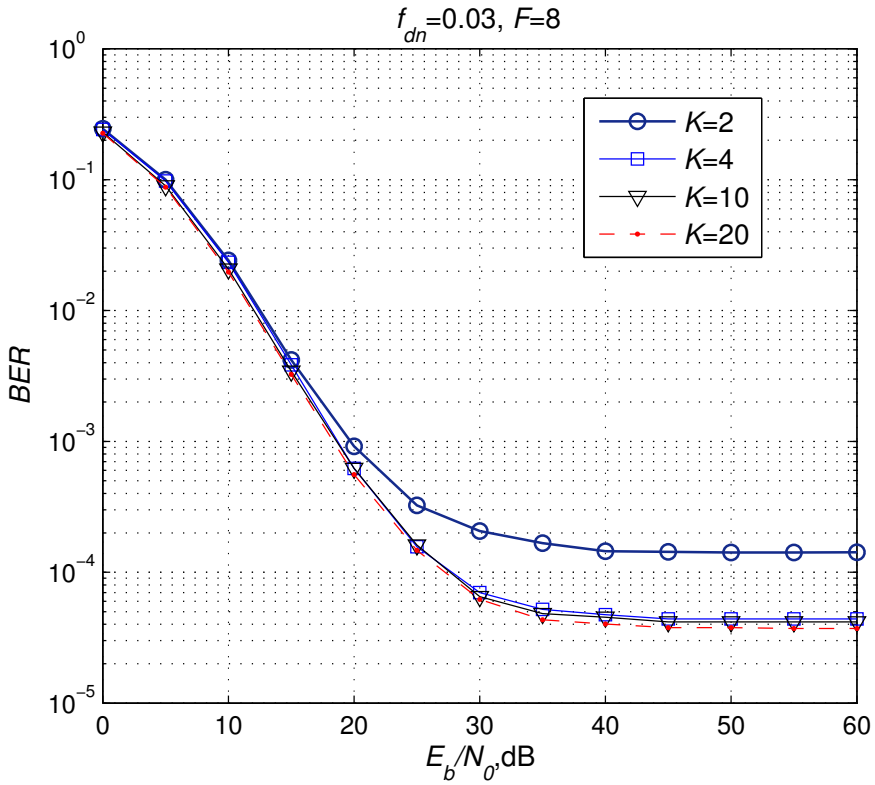

Figure 4.7: The effect of K on the performance of the Alamouti encoded systems with BPSK constellation, $f_{dn} = 0.03$.

CHAPTER 5

COMPARISON OF TSTD AND STBC OVER TIME-VARYING MISO CHANNELS

In this chapter, we compare the BER and PER performances of the Alamouti scheme and TSTD both concatenated with a convolutional code over 2x1 time-varying channels. Regarding the time-varying channel as a block-fading channel, we utilized the encoding structures that are designed for the block-fading channels and described in Chapter 3.

In general, time-varying flat-fading channels are modeled as block-fading channels with a finite number of block realizations B in order to develop coding design criteria and exploit the temporal diversity [46]. The approximation in [47] shows that a SISO Rayleigh fading channel with the Jakes' spectrum provides B degrees of freedom, where

$$B \approx 1 + 2 f_{dn} T_p. \tag{5.1}$$

The channel gain coefficients are considered to be constant for T_p/B symbol durations and then change independently. While the time-variation of the channel provides temporal diversity, it may also lead to degradation in error performance, especially at high SNR as explained in Chapter 4. For different f_{dn} and T_p values, Monte Carlo simulations are performed and the error performances of the transmit diversity schemes over Rayleigh fading channels with the Jakes' spectrum are presented in this chapter where the CSI is assumed to be either perfectly known or not available at all at the receiver. The simulations illustrate both improving and detrimental effects of the time-variation on the error performance. The effects of the channel estimation error on the performance of coherent receivers are also provided.

5.1 Coherent Case in Time-Varying Channels

As explained in Section 4.3, inter-antenna interference, which is induced by the linear processing in (2.32), degrades the symbol error performance of the coherent Alamouti scheme even if the channel gain coefficients are perfectly available at the receiver. Note that TSTD does not suffer from this phenomenon, since the symbol decisions are obtained using one symbol observation. Motivated from the difference of the schemes on the susceptibility to the time-variation, the Alamouti scheme is expected to fall behind TSTD in time-varying channels with high f_{dn}. Therefore we investigate the error performances of the transmit diversity schemes in time-varying channels with high f_{dn} when the CSI is perfectly available at the receiver.

In Figures 5.1 and 5.2, the simulation results for the performances of the Alamouti scheme and TSTD with BPSK and QPSK are depicted respectively. The generator polynomial of the rate-1/4 convolutional code is $(3, 5, 7, 7)_8$. This code is in the family of full-diversity achieving codes over SISO block-fading channels with 4 block realizations [25].[1] We fix $f_{dn} = 0.0125$ and $T_p = 40$ in order to satisfy $B = 2$. It is seen in the figures that the difference between the BER (and PER) performances of the Alamouti scheme and TSTD is fraction of a dB for both constellations, resembling the affinity of the error performances of the schemes in block-fading channels.

Figure 5.3 depicts the error performances with $f_{dn} = 0.016667$ and $T_p = 60$ corresponding to $B = 3$ and with BPSK constellation. The generator polynomial of the rate-1/6 full-diversity achieving convolutional code is $(3, 5, 7, 3, 5, 7)_8$ [26]. In Figure 5.4 the same comparison is shown for QPSK. The performance results for the transmit diversity techniques are very close to each other. Note that both schemes approximately achieves the full spatio-temporal diversity order of 6.

In Figures 5.1, 5.2, 5.3, and 5.4, it is seen that the error floors for the PERs cannot be observed up until $PER = 10^{-5}$, although f_{dn} values are relatively high, i.e., 0.013 and 0.017. It is expected with the larger constellations that the Alamouti scheme will suffer from the time-variation of the channel gain coefficients, since the distances of the elements in the con-

[1] Note that a 2x1 BF channel with 2 block realizations is equivalent to a SISO channel with 4 block realizations in a TSTD system.

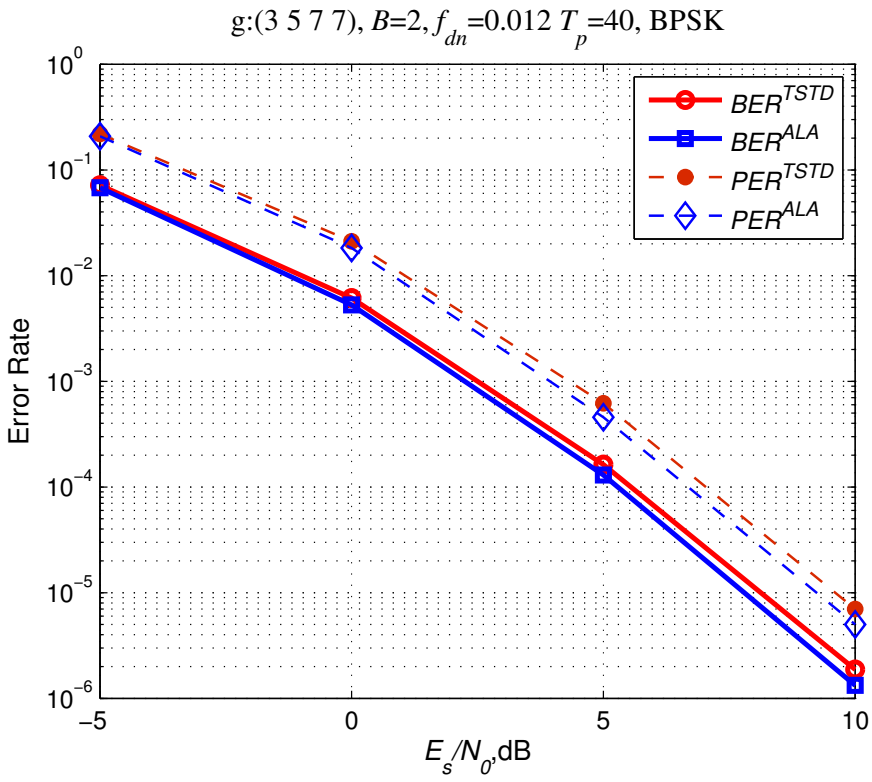

Figure 5.1: B = 2, rate-1/4 convolutional code with generator polynomial (3,5,7,7), T_p = 40, time-varying 2x1 channel, BPSK

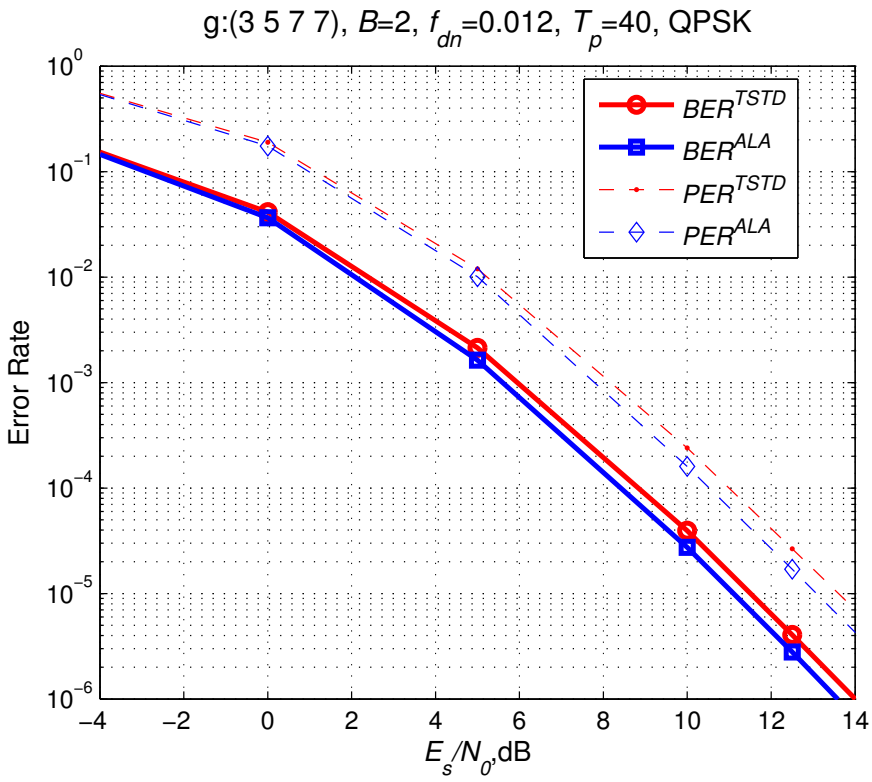

Figure 5.2: $B = 2$, rate-1/4 convolutional code with (3,5,7,7), $T_p = 40$, time-varying 2x1 channel, QPSK

stellation will decrease. However, it is observed in the undocumented simulation results that a significant error floor of the PER does not occur with M-PSK constellations, $M < 32$, still until $PER = 10^{-5}$. Note that the TSTD technique is not also adversely affected by the time-variation.

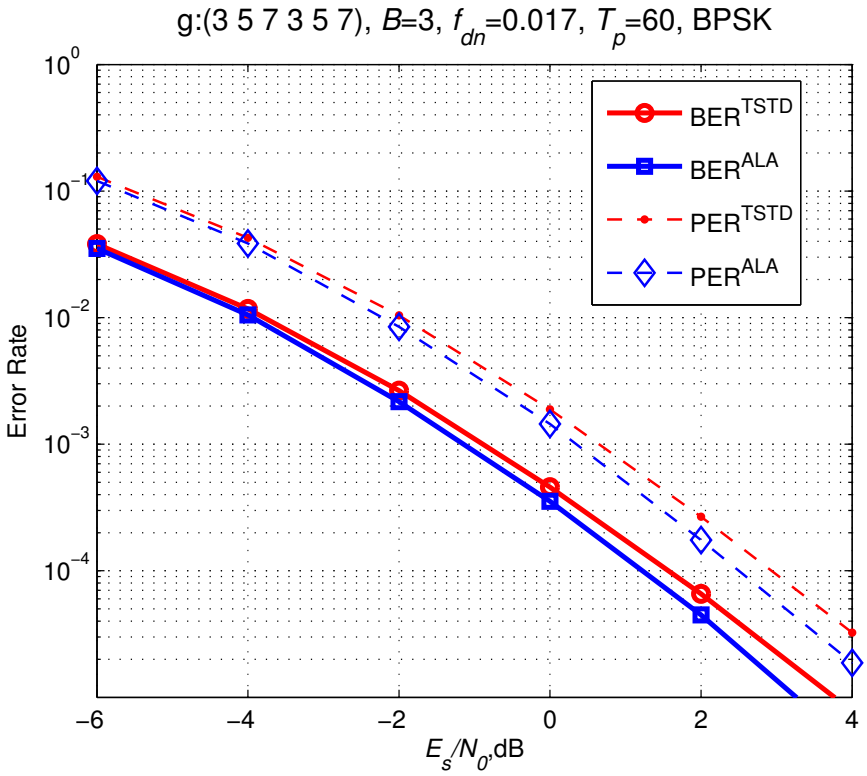

Figure 5.3: $B = 3$, rate-1/6 convolutional code with (3,5,7,3,5,7), $T_p = 60$, time-varying 2x1 channel, BPSK

In Section 4.2 it is shown that the channel estimation error degrades the error performance of the Alamouti scheme. In order to compare the Alamouti scheme and TSTD both with concatenated coding under channel uncertainty, the BER and PER performances of the transmit diversity schemes where the channel gain coefficients are obtained with the aid of the PSAM technique are depicted in Figure 5.5. In the simulations we fix $f_{dn} = 0.0125$, $\gamma_p = 1$, and $F = 10$. In order to investigate the effects of the channel estimation error on the error performances at high SNR, γ_p is kept constant, independent of γ_s.

Here, how the placement of the pilots will be done is a complicated question. Since T_p is finite, the channel gain coefficients near the edges of a packet are estimated more erroneously

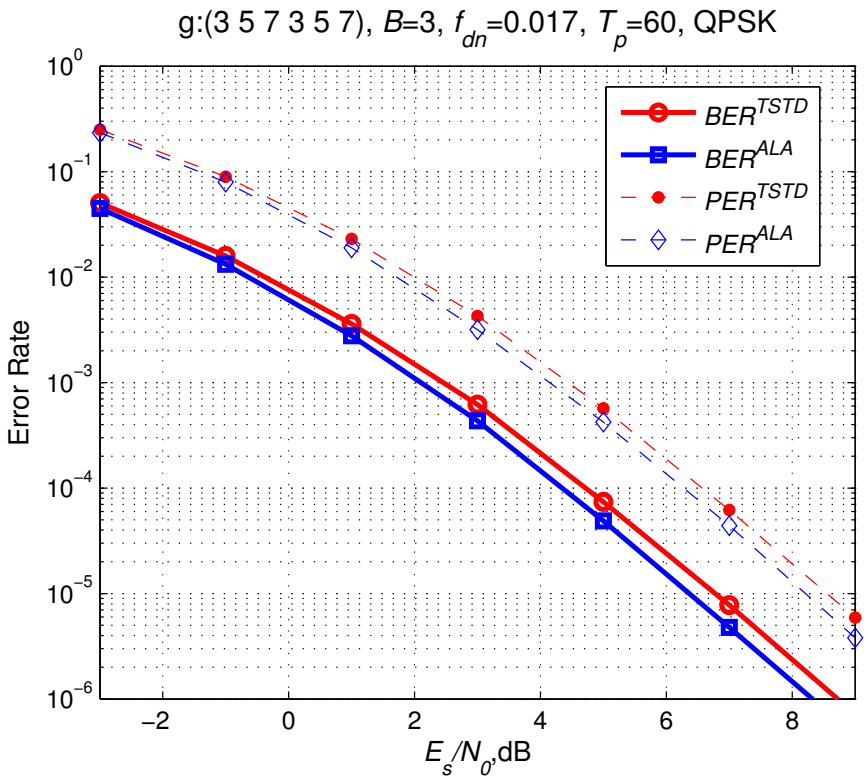

Figure 5.4: B = 3, rate-1/6 convolutional code with (3,5,7,3,5,7), T_p = 60, time-varying 2x1 channel, QPSK

if the pilots are uniformly distributed, i.e., equally spaced, throughout the packet. In this case the pilots may be distributed such that more pilots are inserted near the edges of the packet as in [48]. By this way the estimation error of the channel gain coefficients near the edges will decrease. However, the optimization of the pilot placement seems to be cumbersome. Therefore, the channel gain coefficients and the estimation errors are generated using the power spectrum densities (PSD) of the random variables assuming the parameters above are valid. The pilots are assumed to be uniformly distributed and the interpolator number K is assumed to be infinite. The PSD's can be found in [39].

Using (4.11), we deduce that the PSAM parameters lead to a ξ_{min} of 0.192. The parameter f_{dn} and $T_p = 40$ are chosen so that $B = 2$ and the generator polynomial of the rate-1/4 convolutional code is $(3, 5, 7, 7)_8$. Note that the induced error floor of the Alamouti scheme is larger than the error floor of the TSTD technique.

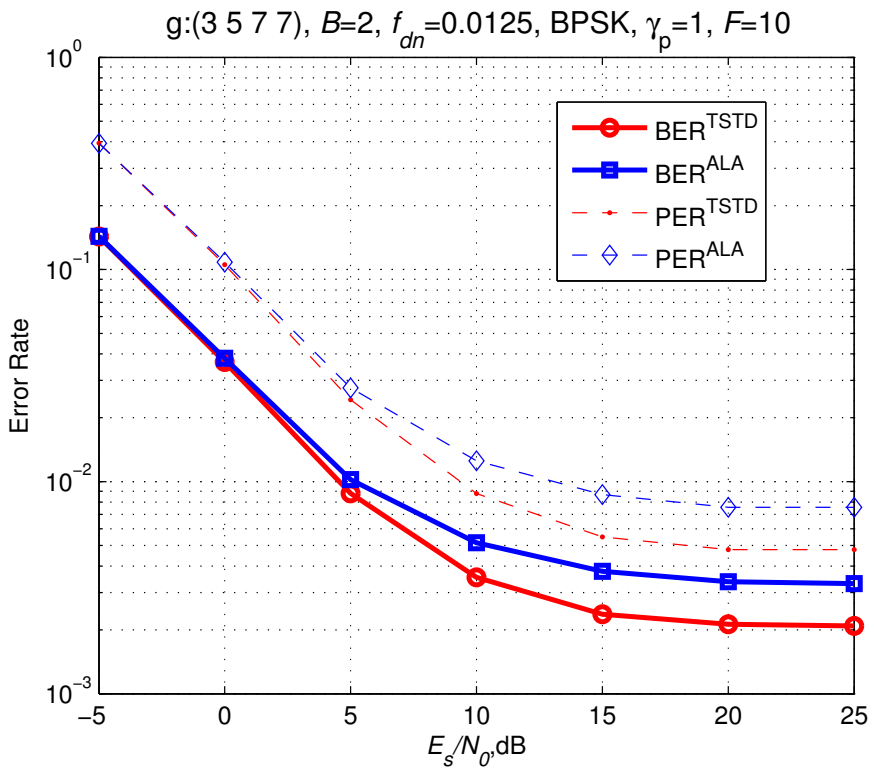

Figure 5.5: The effects of channel estimation error and time-variation on the performances of both transmit diversity schemes where the channel gain coefficients are estimated via the PSAM technique.

5.2 Noncoherent Case in Time-Varying Channels

In this section the comparison of the TSTD technique with DPSK and DSTBC where no CSI available at the receiver is given. The encoding/interleaving and receiver structures are explained in Chapter 3.

It is demonstated in Section 4.6 that time-variation degrades both the error performances of DPSK and DSTBC. In DPSK two adjacent channel gain coefficients are assumed to be equal, whereas the channel gain coefficients in DSTBC are assumed to be constant for 4 symbol durations. The correlation coefficient between two adjacent channel gain coefficients corresponding to the same antenna in a time-varying MISO channel with Jakes' spectrum is 0.9961 when $f_{dn} = 0.02$. The correlation coefficient equals 0.9648 when the channel gain coefficients are separated by 3 symbol durations. Besides, the two-symbol observation ML symbol receiver[2] for uncoded DPSK over time-varying channels is equivalent to the case with quasi-static channel [49]. However, ML receiver for uncoded DSTBC can be derived from (2.42) and is not equivalent to the receiver over quasi-static channel. Therefore DSTBC is expected to be more susceptible against time-variation than TSTD with DPSK is.

In Figure 5.6 the simulation results for $f_{dn} = 0.020833$, $T_p = 24$, and $B = 2$ are depicted. Since the comparison is done with high f_{dn} and $B = 2$, such a small value of T_p is chosen according to (5.1) which is actually impractical. The bits are coded with a rate-1/4 convolutional code having the generator polynomial $(3, 5, 7, 7)_8$, and modulated with 8-PSK constellation. Note that the performance results are almost the same. The error floor is not observable in the range of display even with a relatively high f_{dn} and a moderately large PSK constellation.

When the coding rate of the outer channel code increases, the performances of the transmit diversity techniques are expected to deteriorate. In order to observe the detrimental effects of time-variation, the rate of the outer channel code is increased to 1/2 over a 2x1 time-varying channel with $B = 4$, $f_{dn} = 0.03125$, and $T_p = 48$. Using (3.8) and (3.9), it can be seen that TSTD can achieve a diversity order of 5 whereas the Alamouti scheme can achieve a diversity order of 6 on an equilavent block-fading channel. The convolutional code having the generator polynomial (26,74) is used, which achieves the Singleton bound (3.6) on a SISO block-fading chanel with $B = 8$. Note that the outer channel code that achieves the Singleton bound (3.8)

[2] Classical DPSK receiver

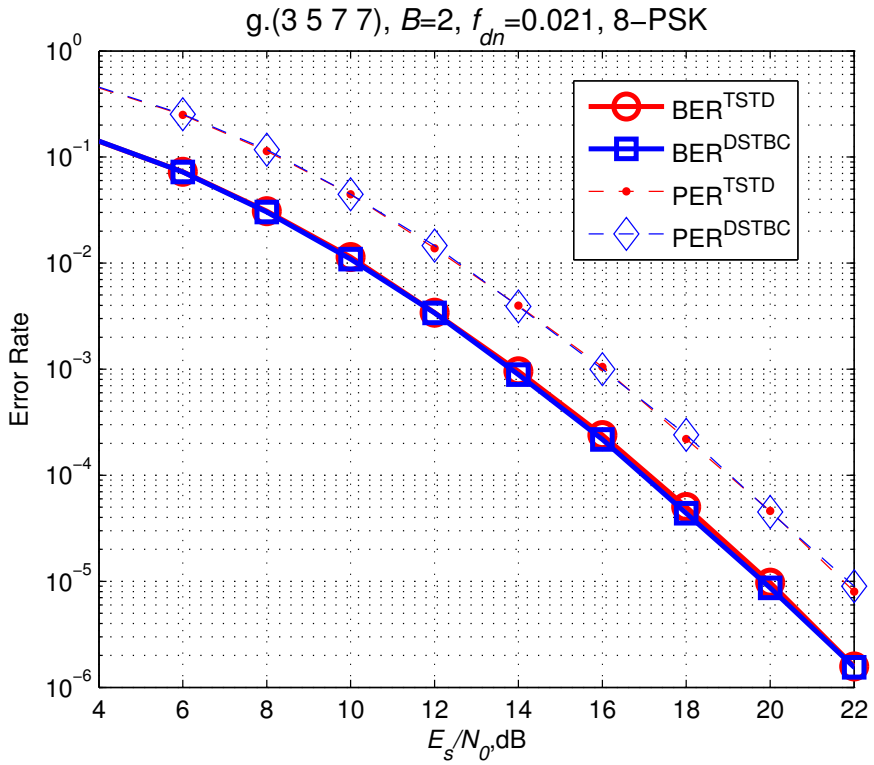

Figure 5.6: B = 2 rate-1/4 convolutional code (3,5,7,7) T_p = 24 8-PSK

with TSTD, also achieves (3.9) with the Alamouti scheme as explained in Section 3.4. In Figure 5.7, the transmit diversity schemes are compared with BPSK constellation. Enjoying the diversity advantage over TSTD, DSTBC have a better error performance.

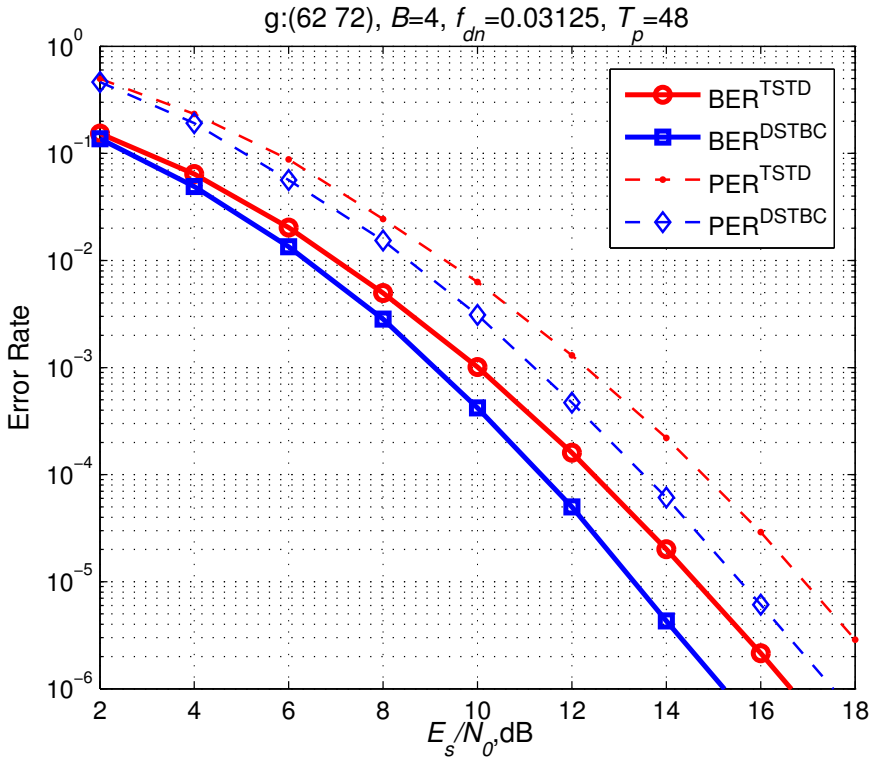

Figure 5.7: $B = 4$, rate-1/2, convolutional code (62,72), $T_p = 48$, BPSK

In Figure 5.8, the schemes are compared with QPSK. Since the distances between the elements of the QPSK constellation are smaller than that of BPSK, QPSK is more susceptible to time-variation in both differential schemes, more intensely in DSTBC as explained before. It is seen that TSTD scheme outperforms DSTBC at SNR values higher than 19 dB.

To see the effects of even higher rate convolutional codes, we present the simulation results for a rate 5/8 outer code. The outer code is not known to guarantee (3.8) and (3.9). Since the rate is rather odd, no Singleton bound achieving code could be found in the literature. In Figures 5.9, 5.10, and 5.11 the performance results of the DSTBC and TSTD over 2x1 time-varying channel with $B = 4$ are depicted for different f_{dn} values. The transmit diversity schemes are concatenated with a 5/8 convolutional code. The output bits corresponding to

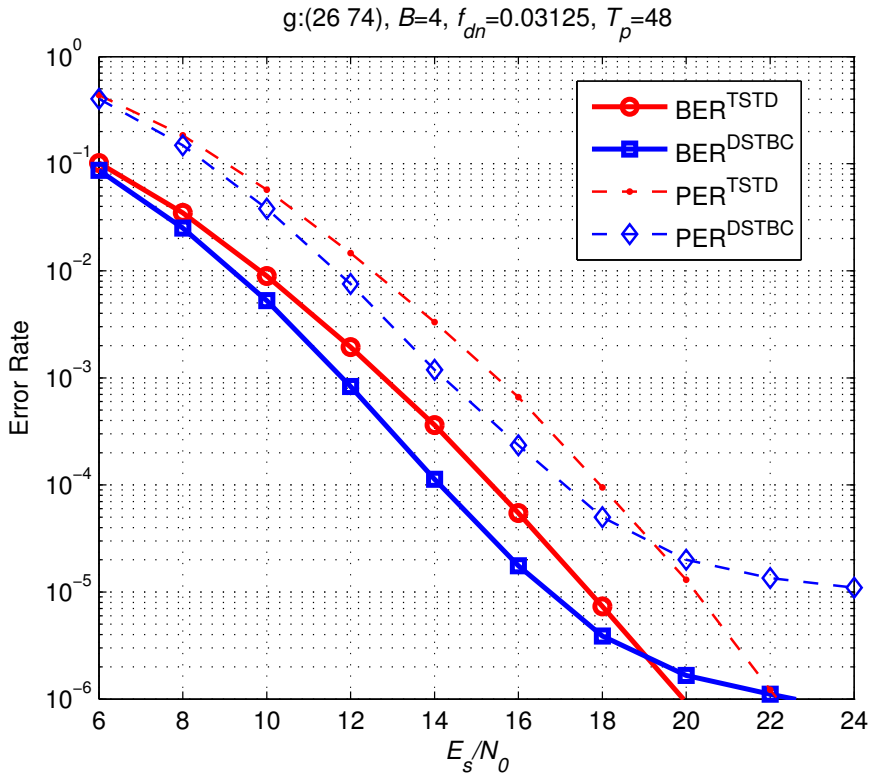

Figure 5.8: $B = 4$, rate-1/2 convolutional code (26,74), $T_p = 48$, QPSK

a state transition in the trellis are sent from different channel realizations. The generator polynomial of the convolutional code is [50]

$$\begin{pmatrix} 320 & 026 & 213 & 034 \\ 116 & 270 & 065 & 377 \end{pmatrix}. \tag{5.2}$$

The constellation set is chosen as 8-PSK. Note that both systems achieve at most a diversity order of 4 on an equilavent block-fading channel, as illustrated in Figure 3.4.

In Figure 5.9 f_{dn} equals 0.017045 and $T_p = 88$. The error performances of the systems are equal to each other at 35 dB SNR. Below this SNR value DSTBC outperforms the TSTD technique with DSTBC having roughly a 4 dB better performance at 10^{-3} PER. When f_{dn} is increased to 0.023438 with $T_p = 64$, DSTBC outperforms the TSTD for $E_s/N_0 < 23$ dB as demonstrated in Figure 5.10. However the error floor of DSTBC is higher than the error floor of TSTD. The error performances with $f_{dn} = 0.03125$ and $T_p = 48$ are illustrated in Figure 5.11. Clearly TSTD has better performance.

Considering the figures it can be deduced as f_{dn} increases that TSTD becomes more advantageous than DSTBC scheme with respect to the error performance.

5.3 Further Results

Lastly, we compare the transmit diversity schemes in a large message size over 2x1 time-varying channels. The outer convolutional codes are judiciously chosen with respect to their free distances d_{free}. The B values are chosen as 32 or 64 and the packet length T_p is 640. The interleaver for the Alamouti scheme is as follows. The output bits corresponding to a state transition in the trellis of the convolutional code is transmitted at different block realizations. In TSTD, the output bits are transmitted at different block/antenna realizations as explained in Chapter 3. Thus TSTD achieves a diversity gain of d_{free} whereas the diversity order of the Alamouti scheme is expected to be $2d_{free}$.

In Figure 5.12 TSTD and the coherent Alamouti scheme are compared where CSI is perfectly available at the receiver. The parameters are chosen as $B = 16$ and $f_{dn} = 0.011719$.

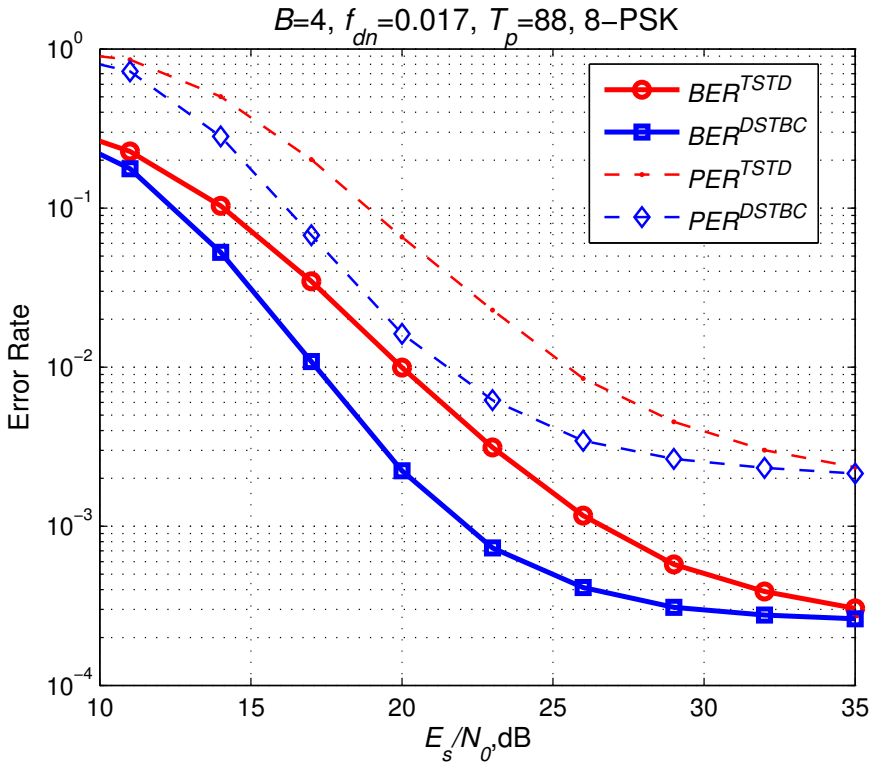

Figure 5.9: $B = 4$ rate-5/8 convolutional code $T_p = 88$ 8-PSK

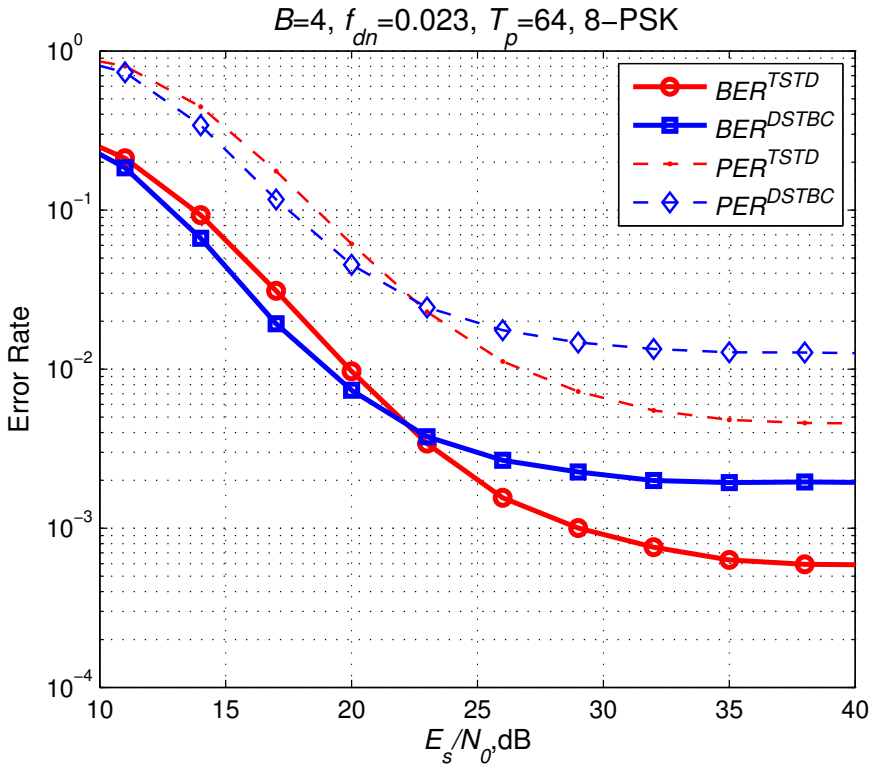

Figure 5.10: $B = 4$ rate-5/8 convolutional code $T_p = 64$ 8-PSK

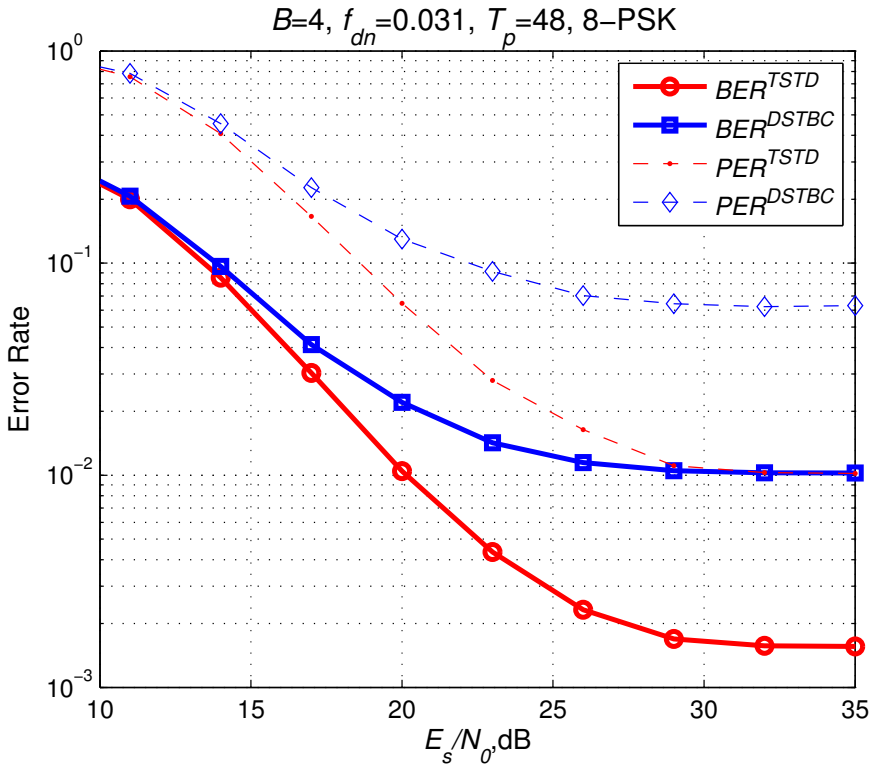

Figure 5.11: $B = 4$ rate-5/8 convolutional code $T_p = 48$ 8-PSK

The schemes are concatenated with a (54,74) convolutional code. The free distance of the convolutional code is 6.

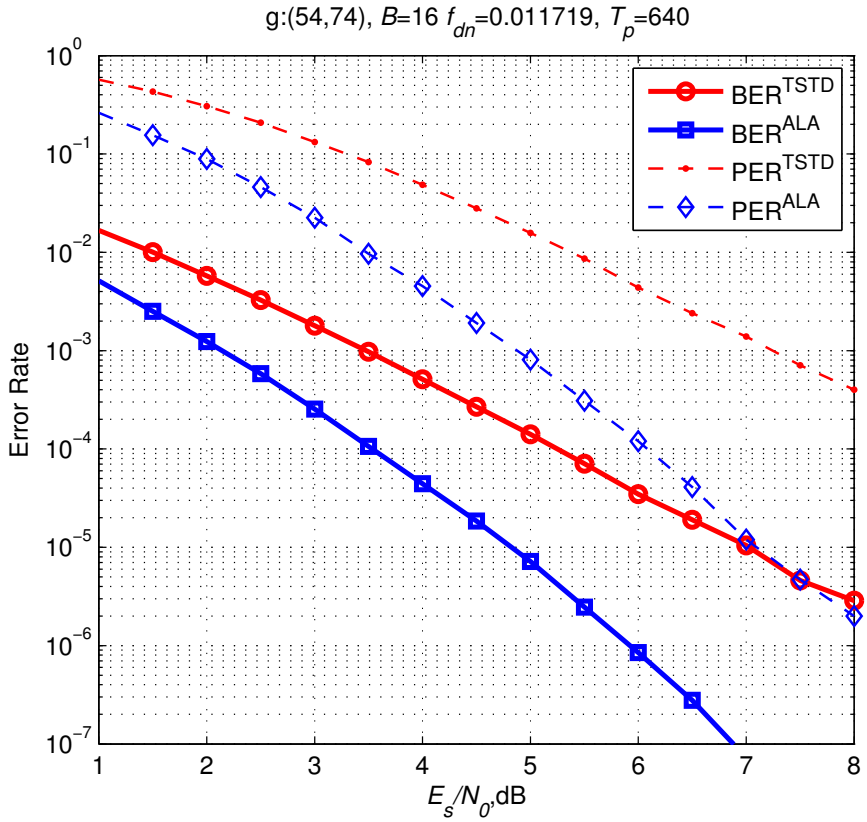

Figure 5.12: $B = 16$ rate-1/2 convolutional code (54,74) $T_p = 640$ BPSK

In Figure 5.13 a (551,641) convolutional code is used. The free distance of the code is 10.

In Figures 5.14 and 5.15 rate-1/2 convolutional codes with generator polynomials (554,774) and (64,74) are used respectively. The CSI is not known at either side. While the expected diversity orders are approximately achieved with coherent receivers, TSTD with DPSK and DSTBC cannot achieve the expected diversity. This phenomenon is another topic of study.

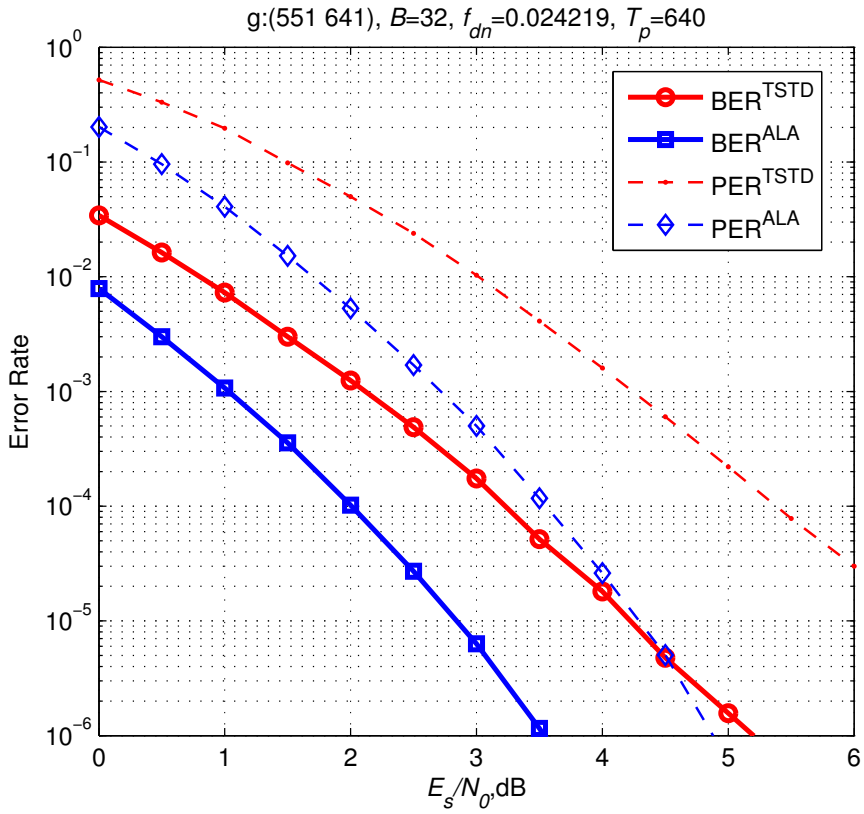

Figure 5.13: B = 32 rate-1/2 convolutional code (551,641) T_p = 640 BPSK

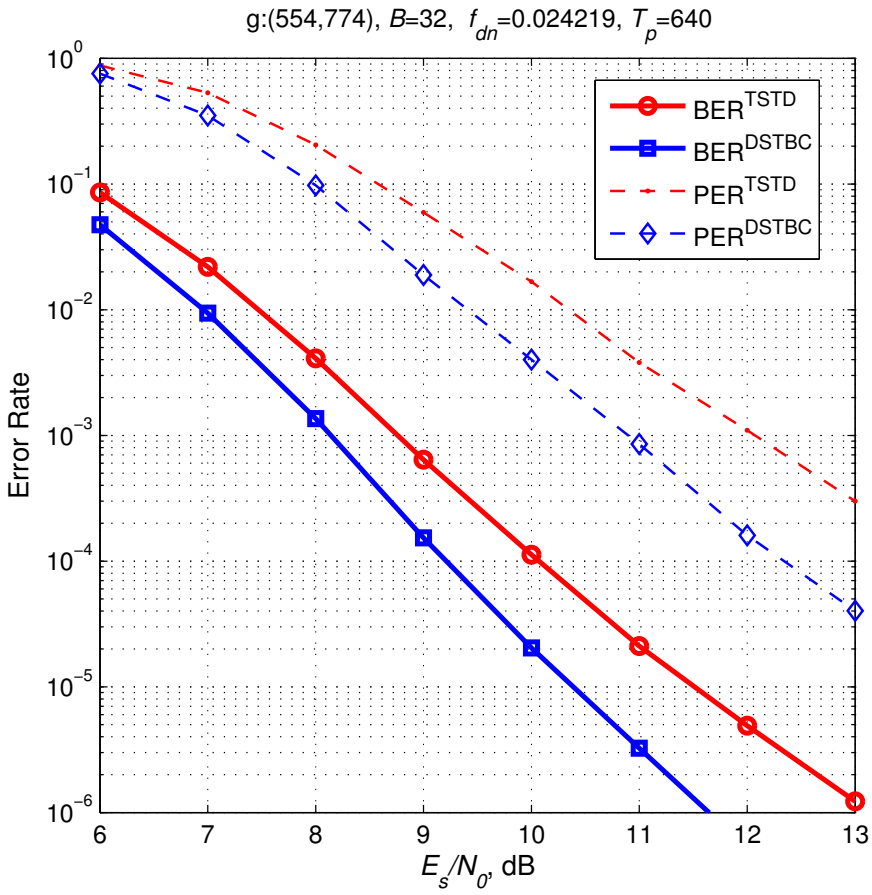

Figure 5.14: $B = 32$ rate-1/2 convolutional code (554,774) $T_p = 640$ QPSK

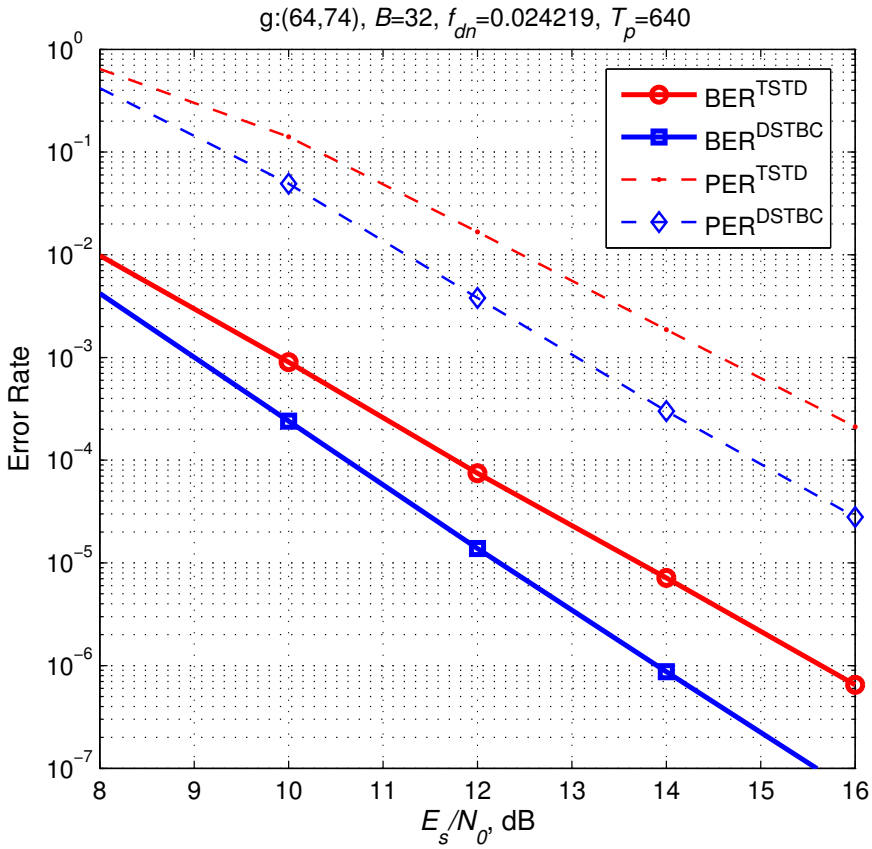

Figure 5.15: $B = 32$ rate-1/2 convolutional code (64,74) $T_p = 640$ QPSK

5.4 Additional Notes

Several techniques aiming to achieve temporal diversity over a time-varying channel are also proposed in the literature. For example, temporal diversity is exploited with the aid of linear constellation precoding as in [51]. With the techniques in [52], the spatio-temporal diversity is turned into frequency diversity with the aid of digital phase sweeping and FFT matrices. The temporal diversity achieving differential coding schemes are given in [53] and [54]. The main idea behind the schemes is to use differential diagonal unitary space-time modulation [19], by regarding the block realizations in time as antenna realizations.

The error performances of the differential schemes can be improved with multiple symbol differential detection (MSDD) [55] or decision feeedback detection (DFD) on time-varying channels. While the techniques yield coding gain and reduce the error floor, they lead to extra decoding complexity. A comprehensive survey can be found in [49] for SISO channels and in [56] for differential unitary signaling in MIMO channels. Futhermore iterative systems are also proposed for differential schemes [57].

CHAPTER 6

CONCLUSIONS AND FUTURE WORK

In the thesis we compared the space-time codes and TSTD over block-fading and time-varying channels with various channel parameters. The thesis includes some basic information about the space-time codes and the TSTD technique and the elaboration on the PSAM technique over time-varying MIMO channels. Furthermore, the detrimental effects of the channel estimation error and time-variation on the Alamouti scheme and TSTD are investigated. The performance analysis of the DSTBC and TSTD with DPSK over time-varying channels are also provided.

It is shown in Chapter 3 that TSTD, being a simply implemented system, has a similar error performance with the Alamouti scheme in block-fading channels when the concatenated code has a coding rate of $1/2B$. The difference between the error performances of the differential counterparts of the schemes are shown to be close to each other. In Chapter 5, the transmit diversity schemes are compared in the time-varying channel with the same channel codes that are used in the block-fading channel and the error performances are seen to be close to each other in this case as well.

It is demonstrated that TSTD can even outperform the space-time codes in some cases. For example, TSTD have a better performance when noisy channel estimates are used. Besides, TSTD has a lower error floor than DSTBC which makes TSTD advantageous in fast-fading channels when CSI not available at the receiver. When the results are combined, TSTD, being implemented with only a single RF-chain, can be seen as a good alternative to the space-time codes for which multiple RF-chains need to be utilized.

In the future work, we may derive upper bounds on the error performances of differentially encoded transmit diversity schemes. The performance results may also be analyzed with

different types of outer channels codes, including turbo codes, LDPC codes, etc. The generalization to the multiple antenna case with $N_t > 2$ may be another topic of study.

REFERENCES

[1] E. Telatar, "Capacity of multi-antenna Gaussian channels," *European Transactions on Telecommunications*, vol. 10, pp. 585 –595, 1999.

[2] G.J. Foschini, "Layered space-time architecture for wireless communication in a fading environment when using multi-element antennas," *Bell Labs Technical Journal*, vol. 1, pp. 41 – 59, 1996.

[3] V. Tarokh, N. Seshadri, and A. R. Calderbank, "Space-time codes for high data rate wireless communication: Performance criterion and code construction," *IEEE Transactions on Information Theory*, vol. 44, no. 2, pp. 744–765, 1998.

[4] S.M. Alamouti, "A simple transmit diversity technique for wireless communications," *Selected Areas in Communications, IEEE Journal on*, vol. 16, no. 8, pp. 1451 –1458, Oct. 1998.

[5] H. Olofsson, M. Almgren, and M. Hook, "Transmitter diversity with antenna hopping for wireless communication systems," in *Proc. IEEE 47th Vehicular Technology Conf*, 1997, vol. 3, pp. 1743–1747.

[6] Hamid Jafarkhani, *Space-Time Coding: Theory and Practice*, Cambridge University Press, 2005.

[7] G.B. Giannakis, Z. Liu, X. Ma, and Z. Shengli, *Space-time coding for broadband wireless communications*, Wiley-InterScience, 2007.

[8] V. Tarokh, H. Jafarkhani, and A.R. Calderbank, "Space-time block codes from orthogonal designs," *Information Theory, IEEE Transactions on*, vol. 45, no. 5, pp. 1456 –1467, July 1999.

[9] Haiquan Wang and Xiang-Gen Xia, "Upper bounds of rates of space-time block codes from complex orthogonal designs," in *Proc. IEEE Int Information Theory Symp*, 2002.

[10] H. Jafarkhani, "A quasi-orthogonal space-time block code," *IEEE Transactions on Communications*, vol. 49, no. 1, pp. 1–4, 2001.

[11] N. Sharma and C. B. Papadias, "Improved quasi-orthogonal codes through constellation rotation," *IEEE Transactions on Communications*, vol. 51, no. 3, pp. 332–335, 2003.

[12] H. El Gamal and A. R. Hammons, "A new approach to layered space-time coding and signal processing," *IEEE Transactions on Information Theory*, vol. 47, no. 6, pp. 2321–2334, 2001.

[13] S. Sugiura, S. Chen, and L. Hanzo, "Coherent and differential space-time shift keying: A dispersion matrix approach," *IEEE Transactions on Communications*, vol. 58, no. 11, pp. 3219–3230, 2010.

[14] V. Tarokh and H. Jafarkhani, "A differential detection scheme for transmit diversity," *IEEE Journal on Selected Areas in Communications*, vol. 18, no. 7, pp. 1169–1174, 2000.

[15] Charles R Horn, Roger A.; Johnson, *Matrix Analysis*, Cambridge University Press, 1985.

[16] H. Jafarkhani and V. Tarokh, "Multiple transmit antenna differential detection from generalized orthogonal designs," *IEEE Transactions on Information Theory*, vol. 47, no. 6, pp. 2626–2631, 2001.

[17] T. L. Marzetta and B. M. Hochwald, "Capacity of a mobile multiple-antenna communication link in Rayleigh flat fading," *IEEE Transactions on Information Theory*, vol. 45, no. 1, pp. 139–157, 1999.

[18] Lizhong Zheng and D. N. C. Tse, "Communication on the Grassmann manifold: A geometric approach to the noncoherent multiple-antenna channel," *IEEE Transactions on Information Theory*, vol. 48, no. 2, pp. 359–383, 2002.

[19] B. M. Hochwald and T. L. Marzetta, "Unitary space-time modulation for multiple-antenna communications in Rayleigh flat fading," *IEEE Transactions on Information Theory*, vol. 46, no. 2, pp. 543–564, 2000.

[20] B. M. Hochwald and W. Sweldens, "Differential unitary space-time modulation," *IEEE Transactions on Communications*, vol. 48, no. 12, pp. 2041–2052, 2000.

[21] K. L. Clarkson, W. Sweldens, and A. Zheng, "Fast multiple-antenna differential decoding," *IEEE Transactions on Communications*, vol. 49, no. 2, pp. 253–261, 2001.

[22] J. Bannister, P. Mather, and S. Coope, *Convergence technologies for 3G networks: IP, UMTS, EGPRS and ATM*, John Wiley & Sons, 2004.

[23] C. Johnson, *Radio access networks for UMTS: principles and practice*, John Wiley & Sons, 2008.

[24] Mamadou Thioune Javier Sánchez, *UMTS*, John Wiley & Sons, 2007.

[25] R. Knopp and P. A. Humblet, "On coding for block fading channels," *IEEE Transactions on Information Theory*, vol. 46, no. 1, pp. 189–205, 2000.

[26] H. El Gamal and A. R. Hammons, "On the design of algebraic space-time codes for MIMO block-fading channels," *IEEE Transactions on Information Theory*, vol. 49, no. 1, pp. 151–163, 2003.

[27] M. Chiani, A. Conti, and V. Tralli, "Further results on convolutional code search for block-fading channels," *IEEE Transactions on Information Theory*, vol. 50, no. 6, pp. 1312–1318, 2004.

[28] Y. Kofman, E. Zehavi, and S. Shamai, "nd-convolutional codes. I. Performance analysis," *IEEE Transactions on Information Theory*, vol. 43, no. 2, pp. 558–575, 1997.

[29] G. Caire, G. Taricco, and E. Biglieri, "Bit-interleaved coded modulation," *IEEE Transactions on Information Theory*, vol. 44, no. 3, pp. 927–946, 1998.

[30] J.G. Proakis, *Digital Communications 4th Ed.*, McGraw-Hill, 2001.

[31] Y. S. Leung, S. G. Wilson, and J. W. Ketchum, "Multifrequency trellis coding with low delay for fading channels," *IEEE Transactions on Communications*, vol. 41, no. 10, pp. 1450–1459, 1993.

[32] M. Dekker, *Multidimensional systems: techniques and applications*, 1986.

[33] E. Malkamaki and H. Leib, "Evaluating the performance of convolutional codes over block fading channels," *IEEE Transactions on Information Theory*, vol. 45, no. 5, pp. 1643–1646, 1999.

[34] E. Malkamaki and H. Leib, "Coded diversity on block-fading channels," *IEEE Transactions on Information Theory*, vol. 45, no. 2, pp. 771–781, 1999.

[35] J. K. Cavers, "An analysis of pilot symbol assisted modulation for Rayleigh fading channels [mobile radio]," *IEEE Transactions on Vehicular Technology*, vol. 40, no. 4, pp. 686–693, 1991.

[36] Andrea Goldsmith, *Wireless Communications*, Cambridge University Press, 2005.

[37] S. Ohno and G. B. Giannakis, "Average-rate optimal PSAM transmissions over time-selective fading channels," *IEEE Transactions on Wireless Communications*, vol. 1, no. 4, pp. 712–720, 2002.

[38] A. Lozano, "Interplay of spectral efficiency, power and Doppler spectrum for reference-signal-assisted wireless communication," *IEEE Transactions on Wireless Communications*, vol. 7, no. 12, pp. 5020–5029, 2008.

[39] A. Lozano and N. Jindal, "Optimum pilot overhead in wireless communication: A unified treatment of continuous and block-fading channels," in *Proc. European Wireless Conf. (EW)*, 2010, pp. 725–732.

[40] J. Wu and G. J. Saulnier, "Orthogonal space-time block code over time-varying flat-fading channels: Channel estimation, detection, and performance analysis," *IEEE Transactions on Communications*, vol. 55, no. 5, pp. 1077–1087, 2007.

[41] D. Gu and C. Leung, "Performance analysis of transmit diversity scheme with imperfect channel estimation," *Electronics Letters*, vol. 39, no. 4, pp. 402–403, 2003.

[42] J. Jootar, J. R. Zeidler, and J. G. Proakis, "Performance of Alamouti space-time code in time-varying channels with noisy channel estimates," in *Proc. IEEE Wireless Communications and Networking Conf*, 2005, vol. 1, pp. 498–503.

[43] A. Vielmon, Ye Li, and J. R. Barry, "Performance of Alamouti transmit diversity over time-varying Rayleigh-fading channels," *IEEE Transactions on Wireless Communications*, vol. 3, no. 5, pp. 1369–1373, 2004.

[44] T. A. Tran and A. B. Sesay, "A generalized linear quasi-ML decoder of OSTBCs for wireless communications over time-selective fading channels," *IEEE Transactions on Wireless Communications*, vol. 3, no. 3, pp. 855–864, 2004.

[45] Thian Ping Soh, Pooi Yuen Kam, and Chun Sum Ng, "Bit-error probability for orthogonal space-time block codes with differential detection," *IEEE Transactions on Communications*, vol. 53, no. 11, pp. 1795–1798, 2005.

[46] A. Guillen i Fabregas and G. Caire, "Coded modulation in the block-fading channel: Coding theorems and code construction," *IEEE Transactions on Information Theory*, vol. 52, no. 1, pp. 91–114, 2006.

[47] G. B. Giannakis and C. Tepedelenlioglu, "Basis expansion models and diversity techniques for blind identification and equalization of time-varying channels," *Proceedings of the IEEE*, vol. 86, no. 10, pp. 1969–1986, 1998.

[48] Min Dong, Lang Tong, and B. M. Sadler, "Optimal insertion of pilot symbols for transmissions over time-varying flat fading channels," *IEEE Transactions on Signal Processing*, vol. 52, no. 5, pp. 1403–1418, 2004.

[49] R. Schober, W. H. Gerstacker, and J. B. Huber, "Decision-feedback differential detection of MDPSK for flat Rayleigh fading channels," *IEEE Transactions on Communications*, vol. 47, no. 7, pp. 1025–1035, 1999.

[50] D. Daut, J. Modestino, and L. Wismer, "New short constraint length convolutional code constructions for selected rational rates," *IEEE Transactions on Information Theory*, vol. 28, no. 5, pp. 794–800, 1982.

[51] Yan Xin, Zhengdao Wang, and G. B. Giannakis, "Space-time diversity systems based on linear constellation precoding," *IEEE Transactions on Wireless Communications*, vol. 2, no. 2, pp. 294–309, 2003.

[52] Xiaoli Ma, G. Leus, and G. B. Giannakis, "Space-time-Doppler block coding for correlated time-selective fading channels," *IEEE Transactions on Signal Processing*, vol. 53, no. 6, pp. 2167–2181, 2005.

[53] R. Schober and L. H. J. Lampe, "Differential modulation diversity," *IEEE Transactions on Vehicular Technology*, vol. 51, no. 6, pp. 1431–1444, 2002.

[54] Xiaoli Ma, G. B. Giannakis, and Bing Lu, "Block differential encoding for rapidly fading channels," *IEEE Transactions on Communications*, vol. 52, no. 3, pp. 416–425, 2004.

[55] D. Divsalar and M. K. Simon, "Multiple-symbol differential detection of MPSK," *IEEE Transactions on Communications*, vol. 38, no. 3, pp. 300–308, 1990.

[56] R. Schober and L. H.-J. Lampe, "Noncoherent receivers for differential space-time modulation," *IEEE Transactions on Communications*, vol. 50, no. 5, pp. 768–777, 2002.

[57] P. Hoeher and J. Lodge, "Turbo DPSK: Iterative differential PSK demodulation and channel decoding," *IEEE Transactions on Communications*, vol. 47, no. 6, pp. 837–843, 1999.